

**T.C.  
FATİH UNIVERSITY  
INSTITUTE OF BIOMEDICAL ENGINEERING**

**CALCULATION OF VOLUME CONTRACTION ACCURACY  
BASED ON CT PLAN USING TOMO THERAPY FOR HEAD AND  
NECK CANCER PATIENTS**

**SÜMEYRA CAN**

**MSc. THESIS  
BIOMEDICAL ENGINEERING PROGRAMME**

**İSTANBUL, MAY / 2014**

**T.C.  
FATİH UNIVERSITY  
INSTITUTE OF BIOMEDICAL ENGINEERING**

**CALCULATION OF VOLUME CONTRACTION ACCURACY  
BASED ON CT PLAN USING TOMO THERAPY FOR HEAD AND  
NECK CANCER PATIENTS**

**SÜMEYRA CAN**

**MSc. THESIS  
BIOMEDICAL ENGINEERING PROGRAMME**

**THESIS ADVISOR  
YRD. DOÇ. DR. HAŞİM ÖZGÜR TABAKOĞLU**

**İSTANBUL, MAY / 2014**

**T.C.  
FATİH ÜNİVERSİTESİ  
BİYOMEDİKAL MÜHENDİSLİK ENSTİTÜSÜ**

**TOMOTERAPİ İLE TEDAVİ EDİLEN BAŞ BOYUN KANSERİ  
HASTALARI İÇİN CT PLANINA GÖRE HACİM KÜÇÜLMESİNİN  
DOĞRULUĞUNUN HESAPLANMASI**

**SÜMEYRA CAN**

**YÜKSEK LİSANS TEZİ  
BİYOMEDİKAL MÜHENDİSLİĞİ PROGRAMI**

**DANIŞMAN  
YRD. DOÇ. DR. HAŞİM ÖZGÜR TABAKOĞLU**

**İSTANBUL, MAY / 2014**



*To my family and educators who support me during my education life,*

This study was supported by Radiation Oncology Department, University of California Los Angeles

## **ACKNOWLEDGEMENTS**

I would like to thank Daniel Low, Professor and Vice Chair of Physics Department at University of California Los Angeles, for giving me this opportunity. I would also like to thank Sharon Qi for helping with the data analysis, explaining Tomo Therapy and to handle all process while doing my research. Finally special thanks to my academic advisor Haşim Özgür Tabakođlu for coordinating my research field.

May 2014

Sümevra Can

# TABLE OF CONTENTS

|   | Page |
|---|------|
| LIST OF SYMBOLS.....                                  | x    |
| ABBREVIATIONS .....                                   | xi   |
| LIST OF FIGURES.....                                  | xii  |
| LIST OF TABLES.....                                   | xiv  |
| SUMMARY.....  | xv   |
| ÖZET.....   | xvi  |
| <br>  |      |
| 1. INTRODUCTION                                       |      |
| 1.1 Literature Review.....                            | 1    |
| 1.2 Purpose of Thesis.....                            | 5    |
| 1.3 Hypothesis.....                                   | 5    |
| <br>  |      |
| 2. SECOND CHAPTER                                     |      |
| <br>  |      |
| HEAD AND NECK CANCER                                  |      |
| 2.1.1 Anatomy of Head and Neck Cancer.....            | 6    |
| 2.1.2 What Causes Cancers of the Head and Neck? ..... | 7    |
| 2.1.3 Sign and Symptoms.....                          | 7    |
| 2.1.4 Treatment Methods for Head and Neck Cancer..... | 8    |
| 2.1.4.1 Surgery.....                                  | 8    |
| 2.1.4.2 Chemotherapy.....                             | 8    |

|  |  |    |
|--|--|----|
| 2.1.4.3  | Radiation Therapy.....   | 8  |
| <br>INTENSITY MODULATED RADIATION THERAPY (IMRT) |  |    |
| 2.2.1  | IMRT .....   | 9  |
| 2.2.2  | Advantages and Disadvantages of IMRT.....  | 10 |
| 2.2.3  | Treatment Planning.....  | 11 |
| 2.2.3.1  | Image Acquisition.....   | 12 |
| 2.2.3.2  | Target Delineation.....  | 12 |
| 2.2.2.3  | Inverse Planning .....   | 13 |
| <br>IMAGE GUIDED RADIATION THERAPY (IGRT)        |  |    |
| 2.3.1  | IGRT .....   | 14 |
| <br>HELICAL TOMO THERAPY                         |  |    |
| 2.4.1  | Helical Tomo Therapy .....   | 17 |
| 2.4.2  | Kilo Voltage Computed Tomography (kVCT) versus Mega Voltage Computed<br>Tomography (MVCT)..... | 19 |
| 2.4.3  | Tomo Therapy Planning.....   | 20 |
| 2.4.3.1  | Optimization.....  | 23 |
| <br>3. THIRD CHAPTER                             |  |    |
| <br>MATERIALS AND METHODS                        |  |    |
| 3.1  | Patient Population and Treatment Planning.....   | 26 |



|   |    |
|---|----|
| 3.2 Optimization Process Based on 0-mm Margin Plan.....                       | 27 |
| 3.3 Deformable Image Registration.....  | 29 |
| 3.4 Data Analysis.....  | 31 |
| <b>4. FOURTH CHAPTER</b>  |    |
| <b>RESULTS</b>  |    |
| 4.1.1 Effective Size Test Result.....   | 32 |
| 4.1.2 The Change in Weight, Volume and COM Displacement.....                  | 37 |
| 4.1.3 Dose Comparison between Standard Margin Plan and 0-mm Margin Plan ..... | 40 |
| DISCUSSION.....   | 52 |
| CONCLUSIONS.....  | 55 |
| REFERENCES.....   | 56 |
| CURRICULUM VITAE.....   | 64 |

—

## LIST OF SYMBOLS

---

|          |                |
|----------|----------------|
| $\Gamma$ | Gamma function |
| $\delta$ | Distance       |
| $\Delta$ | Delta function |

## ABBREVIATIONS

---

BOT : Base of Tongue

COM : Center of Mass

CT : Computed Tomography

CTV : Clinical Target Volume

3D-CRT: Three Dimensional Conformal Radiation Therapy

EUD : Equivalent Uniform Dose

GPU : Graphics Processing Unit

GTV : Gross Tumor Volume

IGRT : Image Guided Radiation Therapy

IMRT : Intensity Modulated Radiation Therapy

kVCT : Kilo Voltage Computed Tomography

MLC : Multi-Leaf Collimator

MVCT : Mega Voltage Computed Tomography

PTV : Planning Target Volume

## LIST OF FIGURES

---

|            | Page   |
|------------|--|
| Figure 2.1 | Target delineation: Contouring the organs at risk for one of the patients.....14   |
| Figure 2.2 | Helical Tomo Therapy Unit, Radiation Oncology Department, UCLA.....18  |
| Figure 2.3 | kVCT-kVCT and kVCT- MVCT pair respectively.....20  |
| Figure 2.4 | Delivering dose in concave shape and organ sparing.....21  |
| Figure 2.5 | Dose Volume Histogram- Standard Cumulative Mode Relative.....24  |
| Figure 4.1 | The planned dose for critical structures regarding standard margin plan versus 0- mm margin plan (a) Cord planned dose (b) Left parotid planned dose (c) Right parotid planned dose.....34         |
| Figure 4.2 | The delivered dose for critical structures regarding standard margin plan versus 0- mm margin plan (a) Cord delivered dose (b) Left parotid delivered dose (c) Right parotid delivered dose.....36 |
| Figure 4.3 | The difference in the delivered dose for ROI from 10 patients.....37   |
| Figure 4.4 | Volumetric Changes of ROI from 10 patients during the treatment course...39  |
| Figure 4.5 | The change in the distance between parotid glands from all patients.....40   |
| Figure 4.6 | The difference in delivered dose between standard and 0- mm margin plans for PTV1 .....41  |
| Figure 4.7 | The difference in mean dose between standard and 0- mm margin plan for CTV2. ....42  |
| Figure 4.8 | The difference in mean dose between standard margin plan and 0-mm margin plan for CTV3. ....42   |
| Figure 4.9 | The dosimetric effect of different margins for targets.....43  |

|             |   |    |
|-------------|---|----|
| Figure 4.10 | Tumor coverage and weekly delivered dose during 6 weeks of the treatment course for selective cases. (Patient-3).....   | 44 |
| Figure 4.11 | (a) The volume change of left parotid gland versus delivered dose (b) The volume change of right parotid gland versus delivered dose .....                                    | 45 |
| Figure 4.12 | The dose distribution based on standard margin plan and 0-mm margin plan for selective cases respectively (Patient-4).....  | 46 |
| Figure 4.13 | (a) The change in volume versus delivered dose for PTV1 (b) The change in volume versus delivered dose for CTV2 (c) The change in volume versus delivered dose for CTV3 ..... | 48 |
| Figure 4.14 | The change in COM displacement versus delivered dose for the cord.....  | 50 |
| Figure 4.15 | (a) The change in COM displacement versus delivered dose for left parotid (b) The change in COM displacement versus delivered dose for right parotid .....                    | 51 |

## LIST OF TABLES

---

|           | Page   |
|-----------|--|
| Table 2.1 | Plan parameters for one patient.....23               |
| Table 3.1 | The characteristics of patients.....27               |
| Table 3.2 | Plan parameters based on standard margin plan.....28 |
| Table 3.3 | Plan parameters based on 0-mm margin plan.....29     |

## SUMMARY

---

### CALCULATION OF VOLUME CONTRACTION ACCURACY BASED ON CT PLAN USING TOMO THERAPY FOR HEAD AND NECK CANCER PATIENTS

Sümeyra CAN

Biomedical Engineering Programme

MSc Thesis

Advisor: Yrd. Doç. Dr. Haşim Özgür TABAKOĞLU

This study aims to determine the accuracy of the volume shrinkage for target as well as parotid glands and dose delivery by using weekly CT images based on 0-mm margin plan for head and neck cancer patients and to prove that IGRT is not enough to protect parotid glands by reducing margin.

For this purpose, ten head and neck patients, treated with simultaneous integrated boost on a Tomo Therapy unit, were selected for this study. Two different plans were generated based on standard margin and 0- mm margin. Calculation of volume contraction accuracy for targets and parotid glands was studied.

The mean volume reduction in PTV1 is 3.3 %. The mean volume reduction in right parotid gland is 11.7 %. The mean volume reduction in left parotid gland is 13.5 %. The mean reduction in the distance between parotid glands is 2.2 %.

Head and neck cancer patients undergo many anatomical changes; therefore, reducing margin is not enough to protect parotid glands. Adaptive radiation therapy is necessary for some cases.

**Keywords:** Head and Neck, IMRT, IGRT, TomoTherapy

---

FATIH UNIVERSITY - INSTITUTE OF BIOMEDICAL ENGINEERING

## ÖZET

---

### TOMOTERAPİ İLE TEDAVİ EDİLEN BAŞ BOYUN KANSERİ HASTALARI İÇİN CT PLANINA GÖRE HACİM KÜÇÜLMESİNİN DOĞRULUĞUNUN HESAPLANMASI

Sümeyra CAN

Biyomedikal Mühendisliği Programı

Yüksek Lisans Tezi

Danışman: Yrd. Doç. Dr. Haşim Özgür TABAKOĞLU

Bu araştırma, tümör hacmindeki ve salgı bezlerinin hacmindeki küçülme miktarının hesaplanmasını ve baş boyun kanseri hastaları için 0-mm magrin kullanılan tedavi planlamasına göre haftalık BT görüntüleri kullanılarak verilen dozun belirlenmesini amaçlar.

Bu nedenle tomoterapi ile tedavi edilen 10 baş boyun kanseri hastası analiz edildi. Standart magrin ve 0-mm magrin baz alınarak iki farklı tedavi planlaması yapıldı. Tümör ve salgı bezlerinin hacimlerdeki küçülme miktarı hesaplandı.

Bu sonuçlara göre, PTV1 hacmindeki ortalama küçülme miktarı 3.3%, sağ ve sol salgı bezlerinin hacmindeki ortalama küçülme miktarı sırasıyla 11.7% ve 13.5% olarak hesaplandı. Ayrıca, salgı bezleri arasındaki mesafenin ortalama küçülme miktarı 2.2% olarak belirlendi.

Baş boyun kanseri hastalarında birçok anatomik değişiklikler gözlemlenir. Margindeki azalma salgı bezlerinin korunması için yeterli değildir. Bu nedenle, bazı hastalar için adaptif radyasyon tedavisinin gerekli olduğu kanıtlanmıştır.

**Anahtar kelimeler:** Baş ve boyun kanseri, IMRT, IGRT, TomoTerapi

---

FATİH ÜNİVERSİTESİ -BİYOMEDİKAL MÜHENDİSLİK ENSTİTÜSÜ



# CHAPTER 1

---

## INTRODUCTION

### 1.1 Literature Review

The number of people who are treated by radiation therapy, an alternative technique for cancer treatment, is mushrooming. Intensity Modulated Radiation Therapy, Image Guidance Radiation Therapy and so on are some radiation therapy techniques. According to the research, scientists have obtained successful results in treating tumors by using radiation therapy. Cancer, especially head and neck cancer, is not a nightmare anymore for most patients with the advent of advanced technology.

In the United States, there are 52,140 new cases and 11,460 deaths each year from head and neck cancers based on American Cancer Society figures (Jemal et al. 2010). It is known that people who smoke cigarettes and drink alcohol have a high risk to become a head and neck cancer patient <sup>1</sup>.

Head and neck cancers are located in the paranasal sinuses, nasal cavity, oral cavity, pharynx and larynx. This type of cancer is mostly seen adjacent to the spinal cord, brain stem, parotid glands and optic pathway. It is also known as squamous cell carcinoma and includes epithelial malignancies. This cancer can be treated with surgery, chemotherapy and radiation therapy. After the delivery of radiation treatment, the long-term survival rate for head and neck cancer patients shows different variations. In this study, radiation therapy is considered specifically as a treatment technique for this type of cancer <sup>2-3</sup>.

Radiation therapy gained its momentum with cutting-edge technology. Before 1990, radiologists used conformal radiotherapy techniques. With the use of this technique, the ability to target the tumor is improved. At the same time, its use can increase the ability to spare normal tissues that are close to tumor locations during treatment

delivery. After 2000, intensity modulated radiation therapy - IMRT - began to be used more widely. Since IMRT decreased xerostomia (dry mouth and symptoms of dryness in the mouth based on changes in the salivary glands after radiation therapy) and increased the long-term quality of life, it has taken the place of conventional radiation therapy (Pow et. al. 2006)<sup>4-5</sup>.

IMRT involves radiation therapy techniques based on the use of a linear accelerator. IMRT improves the therapeutic index by increasing target volume coverage using inverse planning technique for optimization process while reducing doses to the surrounding organs at risk such as the spinal cord and brainstem. In addition, this technology is applied using non-uniform beam intensities therefore delivering the dose with high conformity<sup>6</sup>. Another advantage of IMRT is that it can protect organs at risk during treatment. The organs receive lower doses with this technique<sup>7</sup>. However, it is almost impossible to spare all organs therefore dose accumulation can occur in some. During dose delivery, the radiologist has to choose to protect the smaller organs because it is easier to spare them. At the same time, IMRT allows the radiation oncologist to deliver the dose in a concave shape, and this is why this technique is useful to treat head and neck cancers due to their complex structure<sup>8</sup>. One important concern arises while using this treatment method. Even though IMRT provides target coverage and can spare normal tissues, quality assurance has to be provided. Therefore the planning of the intensity modulated radiation therapy is one of the most crucial aspects of treating this cancer.

There are three different stages of treatment planning. Image acquisition is the first step. Since the tumor location has to be determined with certainty, computed tomography is used to take high-quality images to achieve this goal. After obtaining the first images, physicians have to do target delineation by defining the primary tumor and nodal target on the CT images. During the target delineation process, the gross tumor volume of the primary tumor and the clinical tumor volume have to be taken into consideration on each serial CT scan image. The clinical target volume has to include the gross tumor volume and nodal stations that have organs at risks. Tumor targets and some critical structures such as the brainstem and spinal cord are contoured on slice-by-slice CT images to prevent the mistake of installation of a clinical target volume (CTV). To complete the target delineation process,

physicians have to determine the actual dose for each structure that is contoured. Since organs at risk have specific tolerances, dose limitations should be considered throughout delivering the treatment. The final step of IMRT planning is to establish the specific beam arrangement and to develop dosimetry based on an inverse planning system<sup>9-10</sup>.

Even though intensity modulated radiation therapy provides dose conformity and sparing of vital organs located near the tumor, it has several disadvantages such as longer treatment time and dose inhomogeneity within the target<sup>11</sup>. Additionally, the alteration of tumor location cannot be detected with IMRT. To overcome this obstacle, Image Guidance Radiation Therapy has been developed.

Since the position and shape of the tumor and organ at risks cannot be determined for each treatment circumstances, volumetric images should be acquired using IGRT shaded light to solve this problem and to obtain images with high resolution.

Imaging is the one of the cornerstones of radiation therapy. To prevent setup error, physicians began to use IGRT. It provides two or three-dimensional imaging and decision making at the same time, throughout the course of radiation treatment. The imaging coordinates of the actual treatment plan is made useful for direct radiation therapy. During the radiation treatment course, set-up error, organ motion, as well as a change in the volume and shape of the tumor due to the loss of weight can all occur. To observe these kinds of changes, volumetric images should be acquired. Therefore, the main goal of IGRT is to prevent the uncertainty caused by organ motion and so on by figuring out the patient's anatomical changes. So altering the patient's position and adaptive radiation therapy based on daily or weekly images are made possible by using image guidance radiation therapy (Korreman et al. 2010)<sup>12</sup>. At the same time, verification of actual delivered dose is achieved by increasing confidence and safety<sup>13</sup>. Image guidance radiation technology applies on kilo voltage CT- kVCT and mega voltage CT- MVCT imaging in order to be sure the patient position in all dimensions is accomplished with MVCT during the treatment. However, kVCT images are more helpful to calculate an actual dose. Since contouring the critical structures and all targets slice by slice on kVCT images is more accurate, kVCT is more informative and it is used for diagnosis. It is especially important for head and neck cancer because of the tumor shape<sup>14</sup>.

As mentioned above, IGRT is a useful tool to obtain three-dimensional images. Since intensity modulated radiation therapy does not have image guidance technology, the position and shape of the tumor and OARs cannot be certain with IMRT, so shifting of the location of OARs cannot be observed for each treatment circumstances. As a result, it causes the critical structures such as the spinal cord and parotid glands to receive a higher dose than the actual planned dose. In order to solve this problem, the safety margin can be reduced to maintain the tumor control probability by using IGRT. It is especially important when the tumor is adjacent to critical structures such as parotid glands, spinal cord or brainstem. IGRT makes organ sparing available while delivering a high dose of radiation by increasing safety and reducing the margin<sup>15</sup>. Therefore, for this study, 0-mm margin was applied to protect critical structures as much as possible. To extinguish the uncertainties caused by organ motion, patient's weight and tumor location, some ideas emerged to improve image guidance technology.

There are several treatment methods based on image guidance radiation therapy. Tomo Therapy is the first tool that is used to combine image guidance. Tomo Therapy, meaning, "slice therapy," was invented by Professor Thomas Rockwell Mackie, Ph.D. and Paul Reckwerdt at the University of Wisconsin. The first patients were treated in 2002. Basically, it is a combination of image guidance radiation therapy and intensity modulated radiation therapy. It provides volumetric images by using mega voltage computed tomography (MCVT) because modern CT simulators do not have long acquisition times. MVCT makes motion visualization available to estimate PTV as a target<sup>16-17</sup>. At the same time, it can be easily observed whether or not normal structures encircle the treated volume. Later, this technology was improved by mounting a 6 MV linear accelerator on a ring gantry simulator and was then called helical tomotherapy<sup>18</sup>. Inverse planning is also used for helical Tomo Therapy but a rotational gantry system and binary multi-leaf collimator are promoted instead of a fixed number of beam angles. Two steps- pre-calculation and the optimization stage- are separated in helical Tomo Therapy planning. To optimize patient treatment, the field width with a slice width of 1 cm, 2.5 cm or 5 cm is used based on the jaws- the primary collimator- which are 40 cm wide. In this study, 2.5 cm was chosen as a field width to achieve high dose/ fraction delivery<sup>19</sup>. As a result, delivering a higher dose to

the target while minimizing the dose given to the vital organs is possible.

Since IGRT allows reducing the margin, many scientists have done research in this field, however, this particular proposed research is unique because the 0-mm margin was used for the optimization process based on weekly CT images. In addition, GPU based image framework allows to calculate real time dose accumulation. So, the main goal of this study is to show the benefit of helical Tomo Therapy and image guidance radiation therapy for head and neck cancer treatment. In addition, another primary aim is to protect the salivary glands in order to increase quality of life for those patients who suffer due to xerostomia. Therefore, while doing the optimization process and re-planning the treatment by using CTV, much time was spent on the parotid glands and spinal cord to deliver lower dose than the actual planned dose.

## **1.2 Purpose of Thesis**

The aim of the research is to determine the accuracy of the volume shrinkage for target as well as parotid glands and dose delivery by using weekly CT images based on 0-mm margin plan for head and neck cancer patients treated with helical Tomo Therapy. At the same time, the research aims to reduce the toxicity of delivering high-dose radiation during treatment. In addition, another important goal is to prove that IGRT is not enough to protect parotid glands by reducing margin.

## **1.3 Hypothesis**

IGRT is beneficial tool to reduce margin and correct setup error. However, adaptive radiation therapy is necessary to provide better organ sparing. Therefore, IGRT is not sufficient to protect all OARs by reducing margin. As a result, adaptive radiation therapy should be employed for better protection of parotid glands.

## CHAPTER 2

---

### HEAD AND NECK CANCER

#### 2.1.1 Anatomy of Head and Neck Cancer

Normally, a cell is divided and grows under control. But sometimes it cannot control its growing size, therefore the division begins uncontrollably. As a result, it forms malignant tumors called cancer cells. Some cancer cells may also spread quickly to other body parts. There are more than 200 cancer types defined. Head and neck cancer is one of the most malignant tumors studied in this research specifically.

Head and neck cancer is located in para nasal sinuses, nasal cavity, oral cavity, pharynx and larynx. This type of cancer is mostly seen adjacent to the spinal cord, brain stem, parotid glands and optic pathway. It is also known as squamous cell carcinoma and includes epithelial malignancies. Since head and neck tumors have the ability to penetrate mucosally and submucosally, they can grow quickly.<sup>20</sup>

There are five types of head and neck cancer; oral cavity, pharynx, larynx, paranasal sinuses and nasal cavity, salivary glands. They are classified depending on their origin. Salivary glands are relatively rare compared to other types, while major glands and minor glands located in the oral cavity produce salivary. Also, parotid glands are responsible for the serous secretion. Under certain circumstances, most of the total saliva flow is produced by parotid glands. Since head and neck cancer has a close proximity to critical structure such as parotid glands, cord, brainstem and so on, delivering the radiation therapy without causing a damage to these structures is the most crucial part of treatment. As a result, preserving organ function, especially parotid glands have to be considered to increase quality of life for these patients. According to the research, most of the head and neck cancer patients suffer from xerostomia. Xerostomia is known as dry mouth and symptom of dryness in the mouth due to changing of salivary glands` function after the radiation therapy. If higher dose is delivered to salivary glands, it causes patients to lose their taste and to have difficulties in swallowing. Therefore an alteration occurs in quality of life.<sup>21-22</sup>

### **2.1.2 What causes head and neck cancers?**

There are many reasons causing head and neck cancers, however, it has been proved that people who smoke and drink have a higher risk to have a head and neck cancer, especially cancers of the oral cavity, oropharynx, hypopharynx and larynx.

In the United States, the number of people who are affected by the human papillomavirus (HPV), especially HPV-16 is increasing. This virus causes oropharyngeal cancer particularly. This cancer type includes tonsils or the base of tongue.<sup>23</sup>

In addition to the tobacco smoking, alcohol and HPV, Paan (betel liquid), mate (tea like beverages), conserved or salted food, poor oral hygiene, occupational exposure to wood dust, and exposure to radiation cause the head and neck cancer.

### **2.1.3 Signs and symptoms**

As mentioned before, head and neck cancer spreads quickly due to its nature. This benign tumor is usually seen around lymph nodes in the neck. For the most cases, the tumor location is a crucial sign for certain cancer types such as cancer of the mouth, larynx (voice box), throat, lymphomas and blood cancer. It is often painless and grows rapidly.

According to the origin of head and neck, symptoms might differ. Some changes in voice are the initial sign of larynx cancer. Head and neck cancer located in the mouth can cause a pain or difficulties in swallowing. Sometimes it is painless and it causes bleeding in the late stages of the disease. Blood can be seen in saliva or phlegm. People who have throat or esophagus cancer can have problems while they are swallowing solid food or beverages.

In addition to swallowing problem, patient's skin might be changed because the most common head and neck cancer includes basal cell cancer. Exposure to sun is the most effective cause of basal cell cancer of the skin. Since head and neck region is exposed to the sun more than the other parts of the body, it is especially dangerous for this area. Head and neck cancer mostly includes squamous cell cancer and malignant melanoma; therefore this type of cancer is located on the lower lip and ear. As a result, this malignancy causes a pain around the ear and in the esophagus while swallowing. If this cancer is treated early, it is

not dangerous. Hence, people who have these signs and symptoms should go to a doctor for early detection.<sup>24-25</sup>

#### **2.1.4 Treatment Methods for Head and Neck Cancer**

Before doctors make their decision about which treatment should be used for particular patients, they have to examine them carefully. Treatment methods are determined according to patient's age, tumor location and cancer type. There are three treatment methods; surgery, chemotherapy and radiation therapy.

##### **2.1.4.1 Surgery**

The tumor is removed by the surgeon. If the tumor spreads to lymph node in the neck, surgeon can use surgery as an alternative treatment technique. After the surgery, patient's appearance can be changed. Sometimes, surgery might cause the difficulties of swallowing, talking or chewing.

##### **2.1.4.2 Chemotherapy**

This treatment method is known as anticancer drugs. These drugs have the ability to kill cancer cells as well as blood cells. Since some blood cells play a vital role to kill infections, people might be fatigue against the disease. In addition, some chemotherapy drugs have some side effects. Therefore, patients using these drugs can suffer from diarrhea, vomiting, pain in the mouth and hair loss. Also, these patients might feel themselves tired and they might have joint pains, loss of balance.

##### **2.1.4.3 Radiation Therapy**

Radiation therapy is one of the corner stones for cancer treatment. The use of radiation is necessary for radiation therapy, which is an alternative technique for cancer treatment. Radiation is delivered by an X-ray source with a high energy. When the tumor is exposed to radiation, it is absorbed by the tissue. Therefore it damages the cancer cells by changing their DNA structures. As a result, radiation stops the division of cancer cells.<sup>26</sup>

Although radiation is one of the most effective tools to fight cancer, it has several



undesirable effects as well. Especially head and neck cancer patients suffer from xerostomia, which is related to radiation exposure on parotid glands. After the radiotherapy, these people can lose their taste, which decreases quality of life due to insufficient nutrition. Thus radiation oncology has been improved to reduce these side effects.<sup>24-27</sup>

Today, cancer patients who are treated with radiation therapy have many options to overcome their cancer problem. Intensity modulated radiation therapy and image guidance radiation therapy are some of the most important examples of radiation therapy. Therefore this research aims to show that cancer, especially head and neck cancer, is not a nightmare anymore for cancer patients.

## **INTENSITY MODULATED RADIATION THERAPY (IMRT)**

### **2.2.1 IMRT**

Intensity modulated radiation therapy implies the radiation therapy techniques depending on linear accelerator. It is provided that a tumor can be targeted from different angles by using many small beams or beam lets. Each beam sends the radiation from a specific direction and a computer controls the throughout the radiation treatment course. As a result, radiation is intensified by these beam lets called multi- leaf collimator (MLC). Also, it is possible to block certain areas in the head and neck region during the movement of leaves. The precise dose is delivered to the target and also in specific areas within the target.<sup>28-29-30</sup> In addition, delivering the different doses to multiple targets is possible with only one treatment plan.

IMRT expanded the idea of 3D-CRT to obtain dose conformity for complex tumor shape. It allows the radiation oncologist to deliver the dose in a concave shape, therefore this technique is useful to treat head and neck cancer due to its complex structure. It improves the therapeutic index by increasing target volume coverage and using inverse planning while reducing the delivered dose to the surrounding organs at risk. In addition, computer optimization generates the IMRT plans. This technique is also important to deliver a high dose to the primary target and a lower dose to critical structures.<sup>18</sup> Even though IMRT is a useful tool to provide higher dose conformity, it increases dose inhomogeneity and steep

dose gradient. As a result, the radiation oncologist has to examine carefully the “hot spots” to confirm whether or not they overlap the OARs.<sup>11-19-31</sup>

Since IMRT protects healthy tissues as much as possible against radiation toxicity, it has been used to treat many cancer types such as prostate cancer, head and neck cancer so far. Since head and neck cancer is adjacent to some important organs such as cord, parotid glands, patients diagnosed having this benign tumor can suffer from xerostomia relating to toxicity of parotid glands. As a consequence, sparing the organs at risk is especially important to protect these organ`s function to increase patient`s quality of life.<sup>32-33-34</sup> However, it has limited opportunities to treat breast, thyroid as well as lung cancer.

IMRT application consists of several steps. Immobilization is the most important part of intensity modulated radiation therapy to prevent a set-up error. Since tumor location and size can be changed due to several factors such as loosing weight, imaging and target volume outline have to be determined exactly. For this reason, CT images are used before the treatment course. After obtaining the images, the radiation oncologist should define the dose to be delivered depending on target and they have to consider the critical structures. IMRT is beneficial for plan verification because inverse planning is preferred for IMRT.<sup>35</sup>

### **2.2.2 Advantages and Disadvantages of IMRT**

IMRT has many advantages in treating head and neck cancer; however, it also includes several disadvantages under certain circumstances. IMRT provides target volume coverage by using inverse planning technique while reducing the dose to the surrounding organs at risk such as cord and brainstem.<sup>7</sup> In addition, this technology is applied using non-uniform beam intensities, hence intensity modulated radiation therapy can deliver the dose with high conformity. This is especially important for head and neck cancer because this type of cancer is located adjacent to critical structures. These organs might be given a lower dose with this technique. However, it is almost impossible to spare all these organs. To prevent the invading of critical structures, IMRT might block each beam, so the desired dose is delivered to PTV.<sup>36</sup> In addition, it provides concave shape treatment with this way. As a result, this treatment method is vital for head and neck cancer due to its complex tumor shape. However, blocking each beam causes the dose inhomogeneity in target. But, other

beams can deliver the dose from other directions to increase target volume coverage while sparing OAR. Additionally, it affects steep dose gradient, so a very sharp dose can be observed in IMRT planning.<sup>37</sup> Although IMRT is good at covering the target and sparing the critical structures, longer treatment delivery durations can make patients exhausted. Also, treatment-planning process is time consuming for this treatment technique.

During the radiation treatment course, set-up errors, organ motions, as well as the change in the volume and shape of the tumor due to weight lost might occur. Since intensity modulated radiation therapy does not have image guidance technology, the position and shape of the tumor and OARs cannot be precise with IMRT, and so shifting of the location of OARs cannot be observed on every treatment circumstances. As a result, it causes the critical structure such as cord and parotid glands to receive a higher dose than the actual planned dose due to setup error.<sup>11-38</sup>

### **2.2.3 Treatment Planning**

As explained before, head and neck cancer shows a close proximity to the critical structure. Therefore, treatment planning is the complex part of the treatment. However, according IMRT planning strategies, it has been proved that this treatment method provides organ sparing while delivering the high dose to target volume. According to research, IMRT is effective to protect salivary glands while delivering the radiation. In addition, it is a vital method increasing the patient's quality of life.<sup>4</sup> Even though IMRT provides the target coverage and normal tissue sparing, patient's immobilization is one of the most crucial part. While performing the treatment, a thermoplastic mask provides immobilization. Immobilization is important for the greatest dose conformity.<sup>7</sup> Therefore radiation therapist have to consider daily setup accuracy and the patient's correct position. This is the most challenging part of IMRT treatment plan since the tumor is adjacent to the organs at risk and IMRT shows sharp steep dose gradients between the target and these critical structures. As a result, so much time is spent for an accurate treatment plan.<sup>11-18</sup> IMRT planning includes three steps; image acquisition, target delineation and inverse planning.

### **2.2.3.1 Image Acquisition**

Imaging is one of the corner stones for the radiation therapy. For IMRT planning, patient`s images are obtained by kilo voltage computed tomography before the treatment. For providing daily images to make sure about the patient`s setup and to evaluate the treatment planning, the radiologist prefers to use kVCT for diagnostic purposes. However, MVCT images are used to determine the deformation between kVCT and MVCT images. There is a similarity between them, because their working principle shares the same physics rules called Compton Effect (Ruchala et.al.1999).<sup>39</sup> Compton Scattering is an inelastic one because the momentum and energy cannot be preserved after the interaction. As a result, a decrease in energy and an increase in wavelength occur. Since energy of kVCT and MVCT are different from each other, their interactions with bone and soft tissues are quite different due to Compton effect. Therefore images which are obtained by MVCT are noisier and they have lower contrast than diagnostic kVCT. To conclude, kVCT images are more helpful to calculate the actual dose. Since counteracting the critical structures and all targets slice by slice on kVCT images is more accurate, kVCT is more informative and is used for diagnosis. This is especially important for head and neck cancer because of its tumor shape. Although kVCT makes good diagnostic images available, sometimes MRI and PET scan have to be fused on to CT images to determine the target that is not seen certainly on the CT images and to contour normal structures.<sup>40-41</sup>

### **2.2.3.2 Target Delineation**

After obtaining the first kVCT images, target delineation takes place in IMRT planning as a second step. In this step, determining the gross tumor volume, the clinical target volume and planning target volume is the most vital part. After the physical examination, the first defined volume is the gross tumor volume. Sometimes it encompasses the clinical target volume.

The gross tumor volume gives us information about where the gross diseases are located. The second important volume is the clinical target volume. Clinical target volume includes the gross tumor volume and/or subclinical microscopic malignant disease, which has to be eliminated. It has subdivisions such as CTV1 and CTV2. The high-risk region is

determined under CTV1; however, the low risk region and prophylactically treated neck region are included in CTV2. Therefore, GTV and nodal stations are considered in CTV. Finally, adding safety margin, which can be expanded from 5mm to 20mm, to clinical target volume, forms planning target volume.

In addition, normal structures and some critical structures are contoured in this step.<sup>42</sup> Target delineation is shown in Figure 2.1. The major concern of target delineation is to spare as many healthy organs as possible. It is especially important for parotid glands because total saliva is produced by these glands. Therefore, it is really important to prevent xerostomia linked to radiation toxicity. However, to spare each critical structure is almost impossible. As a result, small organs have to be considered first for sparing. In addition, sometimes reducing margin is beneficial to protect critical structures. It is important when the tumor touches these organs.<sup>1</sup>

### **2.2.3.3 Inverse Planning**

The final step of IMRT planning is to establish the specific beam arrangement and to develop dosimetry according to inverse planning system, which is effective to deliver IMRT.<sup>32</sup> To complete the target delineation process, physicians have to determine the actual dose for each structure that is contoured. Since organs at risk have a special tolerance, dose limitations should be considered throughout performing the treatment. Usually, 70 Gy is given for GTV; however, this delivered dose is less for CTV1 and CTV2. CTV1 may get 66 Gy mostly and at least 54 Gy. 50-54 Gy is appropriate for CTV2.<sup>4</sup> After the specification of desired dose distribution conducted by treatment variables, some calculations about treatment variables have to be done. In this step, the objection function helps the radiation oncologist to find a solution by evaluating the clinical objectives in the form of mathematic. In addition, each iteration calculates the objective function. Eventually, a new dose- volume histogram is obtained according to this inverse planning system.<sup>7-32</sup>

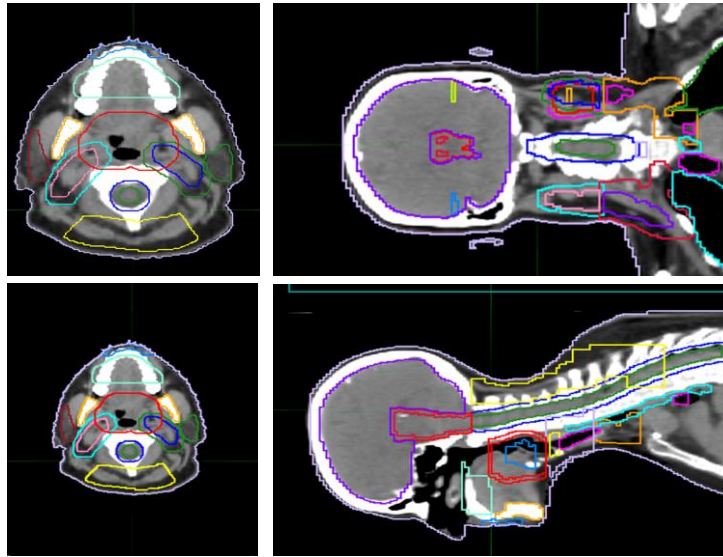


Figure 2.1 Target delineation: Contouring the organs at risk for one of the patients. Based on the picture, dark blue presents mandible. Pink is right parotid glands. Left parotid gland is shown with light blue. Orange is cord. Yellow is chosen for PTV2 and green is chosen for CTV2

## IMAGE GUIDED RADIATION THERAPY (IGRT)

### 2.3.1 IGRT

Imaging is not a new technology developed for medical purposes. The use of medical imaging provides direct visualization of anatomic and physiologic insight into human body. In previous decades, image guidance began to be used in radiation oncology.

It includes different imaging modalities such as photon, electron, and proton external beam therapy. These imaging modalities play an important role to reduce setup errors during the treatment course. In order to obtain an image, 2D and 3D images are used in radiation oncology field.<sup>12</sup>

X- rays are a kind of electromagnetic radiation that was discovered by Wilhelm Rontgen. X- rays have a small wavelength and a high energy; therefore they have a great ability to penetrate in to the object. As a result, X- rays play an important role for medical imaging. Radiograph and computed tomography use X- rays for imaging purposes.

On the other hand, atom ionization occurs when atom is exposed to x- rays due to high energy of X- ray photons. Even though this characteristic of X- rays increases the cancer risk in medical imaging, it is beneficial to kill cancer cell. When X- rays penetrate into the cancer cells, X- ray photons change the function of malignant cell. Since radiation therapy requires high energy, this treatment method uses X- rays to treat cancer patients. Therefore, X- rays are used for radiation oncology for therapeutic purposes.

Since X- ray photons are absorbed by soft tissues, it is beneficial to detect pathology of the skeletal system by radiograph. In addition, these photons are used in order to determine some disease processes in soft tissues. Computed tomography is another tool that uses x- ray photons for diagnostic and therapeutic purposes. Cone beam computed tomography was mounted in linear accelerator to make the image guidance useful in radiation treatment. Tomographic images or the slice of specific region of the body can be obtained by 2- dimensional X- ray images. Since these X- ray images are captured from different directions, they can be utilized into 3- dimensional images inside the body. Therefore computed tomography is beneficial to diagnose and to treat patients.<sup>43-44</sup>

As mentioned above, advent of the IMRT provided and increased quality of life for head and neck cancer patients by sparing OARs and reducing the common toxicity. However, there is a limitation caused by anatomical changes. Since head and neck cancer patients might have significant anatomical changes due to weight loss and volume change of target, it effects the location of some critical structures such as the cord and parotid glands.

In addition, the distance between both parotid glands usually decreases. If parotid glands move to the high dose region, caused by the decrease of the distance, high dose is delivered to the parotid glands.<sup>45</sup> For head and neck cancer patients, increasing the accuracy of the radiation therapy, immobilization and setup correction become more important. Cho et al. described the relationship between the effect of setup uncertainties and equivalent uniform dose distribution.<sup>46</sup> Even though there is a small effect on DVH and EUD when adequate treatment margins are used, reducing margin is especially important when the tumor touches critical structures and geographic miss occurs. Under these circumstances, tumor control probability is not provided. In addition, overdosing of OARs can be observed.<sup>47</sup>

Therefore, radiation therapists have to determine whether there is a shift of OARs before the radiation beam begins to rotate. For this situation, tumor tracking system and re-planning the treatment have become necessary.<sup>15</sup>

Development of the imaging opened a new window to radiation oncology. With the advent of the 3D soft tissue imaging, which can be obtained before, during and after the treatment, detection of the target location and sparing the critical structures such as cord and brainstem become possible. In addition, computed tomography allows the planner to deliver the dose to the target as planned while protecting the normal tissue. Imaging is also essential not only for target coverage and organ sparing but also preventing setup errors due to organ motions. During the radiation treatment, organ motion occurs at esophagus, head and neck region, as well as lungs due to breathing. It causes undesired radiation toxicity.<sup>48</sup> As a result, patient's quality of life decreases. But the advance of imaging overcomes this obstacle by providing good image quality. The change in the position of tumor, an anatomical change due to weight loss might be detected by image guidance technology.<sup>14-49</sup>

Image guidance radiation therapy is one of the most useful tools to provide volumetric images during radiation treatment course. The computed tomography system located on rails can be moved to detect patient's position.<sup>13</sup> Decision making process based on images is possible with this technology. IGRT shed a light by providing the geometric accuracy of tumor location and size. Also, it is possible to detect organ motions. Furthermore, IGRT is beneficial to increase tumor control as well as safety and to decrease toxicity due to radiation.<sup>14-50</sup> As a result, the main concern of IGRT is to provide real time imaging to eliminate uncertainty. One of the goals of IGRT is to allow to change the patient's position and to make the adaptive treatment plan possible. However, the process of IGRT is more complicated and it has several steps. These are;<sup>12</sup>

- ✓ Data acquisition with detection and diagnosis
- ✓ Treatment planning
- ✓ Target delineation and contouring the OARs
- ✓ Dose calculation



Even though IGRT provides volumetric imaging by using mega voltage computed tomography, target localization is the most challenging part because each patient has different changes in their anatomy.<sup>51</sup> Hence, the main goal of IGRT is to prevent the uncertainty caused by organ motion and so by figuring out the patient's anatomical changes. So altering the patient's position and adaptive radiation therapy according to daily or weekly images are made possible by using image guidance radiation therapy (Korreman et al. 2010)<sup>12</sup> Besides, verification of actual delivered dose is achieved by increasing confidence and safety. To conclude, image - guided radiation therapy is crucial to track cancer and to protect normal structures by providing the reduction of margin.<sup>52-53-54</sup>

## **HELICAL TOMO THERAPY**

### **2.4.1 Helical Tomo Therapy**

Tomo Therapy, meaning “slice therapy,” was invented by Professor Thomas Rockwell Mackie, Ph.D. and Paul Reckwerdt at the University of Wisconsin. The first patients were treated in 2002. Tomo Therapy is a combination of image guidance technology and intensity modulation radiotherapy. Basically, a linear accelerator is mounted in a ring gantry. Therefore, this system has the availability to rotate continuously around patients. It delivers the radiation depending on jaws that is the primary collimator.

Jaws are 40 cm wide and it has three different slice width (1cm, 2.5 cm, 5 cm) choices.<sup>16</sup> As a result, Tomo Therapy can produce a finer scan. Also, it is possible to optimize patient treatment. Improving the image quality and changing the length of scan is possible with this technology.<sup>55</sup>

Later, Tomo Therapy was improved by mounting a 6 MV linear accelerator on a ring gantry simulator and was then called helical Tomo Therapy. Figure 2.2 shows helical Tomo Therapy unit at UCLA Radiation Oncology Department. Image guided radiation therapy is also used for helical Tomo Therapy to guarantee patient`s setup by using daily mega voltage computed tomography scan. This system has the ability to rotate 360 degrees around the patient; therefore the radiation is delivered in a helical mode.<sup>56</sup>



Figure 2.2 Helical Tomo Therapy Unit, Radiation Oncology Department, UCLA

Helical Tomo Therapy has multi- leaf collimators. These collimators can switch itself on and off in 20 ms, so they are very fast. Since the number of beam angles per gantry is high, the radiation treatment can be delivered with high intensity modulation.

In addition, the radiation can come from different angles in the rotational gantry system. It allows to deliver the dose in concave shape and to treat multiple targets at the same time.<sup>57</sup> As a result; helical Tomo Therapy is one of the most unique ways to treat head and neck cancer due to its complex tumor structure. This technology also provides a highly conformal dose distribution while sparing organs at risk.<sup>58</sup> Therefore helical Tomo Therapy has several advantages for cancer treatment. First, a high dose can be delivered to the target while reducing the toxicity for critical structures such as cord, parotid glands and brainstem.<sup>59</sup> Second, patient`s position can be corrected before delivering the treatment by using MVCT images. It is especially important for head and neck cancer treatment because patients can lose weight during the treatment course. This change might cause a decrease in distance between parotid gland. So, parotid glands can obtain a higher dose than the actual planned one. As a result, the quality of life will decrease for head and neck cancer patients due to radiation toxicity. This is the unwanted situation. To prevent this condition, the radiation oncologist began to use helical Tomo Therapy to spare OARs as much as possible.<sup>60- 61</sup>

#### 2.4.2 Kilo voltage Computed Tomography (kVCT) versus Mega Voltage Computed Tomography (MVCT)

As mentioned above, Tomo Therapy has high image quality by using mega voltage computed tomography (MVCT). MVCT imaging is a combination of fan beam and helical acquisition paradigm. The use of MVCT is crucial to obtain volumetric images while delivering the treatment to the patient. In this system 3.5 MV X-rays are produced by linear accelerator and photon output is reduced. Photon- efficiency is necessary to obtain volumetric MVCT images.<sup>62-63</sup> The number of photons affects the resolution of image. If the number of photons is high, noise will be reduced. As a result, high contrast will be obtained. Therefore to increase image quality, the number of photons should be increased.<sup>44</sup>

For diagnostic purposes, good image quality has to be obtained to verify the delivered dose. It is also necessary to correct patient` s position.<sup>59</sup> As a result, MVCT makes motion visualization available to estimate PTV as a target. Also, it can be easily observed whether or not normal structures encircle the treated volume.<sup>64</sup> Even though mega voltage imaging provides a good image quality for bony anatomy such as head and neck region, it is not good enough to obtain a high resolution for soft tissues.<sup>44</sup> So, deformation cannot be determined on MVCT imaging due to Compton effect. kVCT is more useful than MVCT in preventing deformation errors and to calculate the dose. Figure 2.3 shows the difference between kVCT- kVCT pair and kVCT- MVCT pair. Since MVCT has a higher X-ray energy, it causes to deliver a more irradiated dose to the patient.<sup>58</sup>

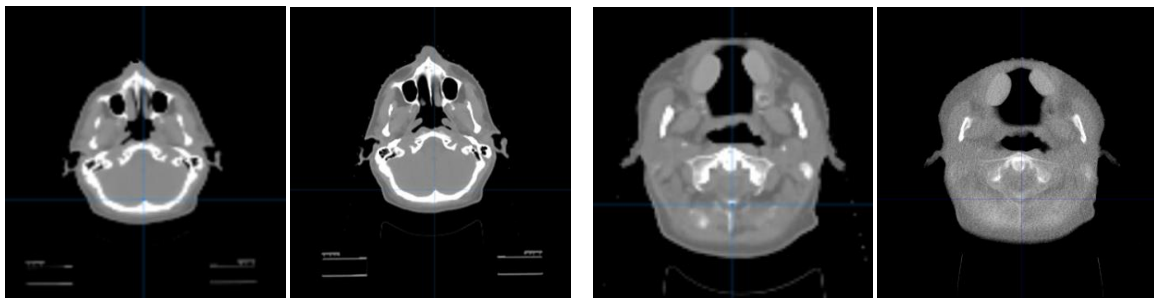


Figure 2.3 kVCT-kVCT and kVCT- MVCT pair respectively

On the other hand, if the patient has significant changes in anatomy during the treatment course, onboard 3D-MVCT has the opportunity to provide adaptive radiation therapy.<sup>65</sup> However, kVCT images were employed for this study because kVCT is crucial for Tomo Therapy planning and it provides accurate results for dose calculation.

### **2.4.3 Tomo Therapy Planning**

Head and neck cancer is located adjacent to critical structures such as spinal cord, brainstem and parotid glands. In addition, tumor location can be changed. Anatomy of head and neck cancer patients can change during the treatment. There are several reasons for this change; patient can lose weight, tumor volume and nodal volume can shrink, the total body mass alteration can occur and the decrease of body fluid can be observed. It can cause the parotid glands to shift towards the primary target. As a result, parotid gland can receive a higher dose than the actual planned one. This unexpected condition prevents the function of parotid glands. After the treatment course, head and neck cancer patients can have problems with salivary production. Furthermore, patient's quality of life can be worse.<sup>66</sup> Because of these reasons, the radiation oncologists have to consider these kinds of problems before delivering radiation. To prevent radiation toxicity, organ deformation has to be detected by using weekly or daily imaging. If organ motion occurs, treatment planning has to be updated according to new target location. It is also important to deliver the exact dose to the planning target volume.<sup>59-67</sup> Even though MVCT is good enough to show anatomical details for bony region, kVCT should be used for dose calculation. On the other hand, the update of treatment plan is not conceivable enough to deliver the actual dose to the critical structures.<sup>45-68</sup> However, Tomo Therapy is a beneficial tool to spare organs at risk as much as possible while delivering the actual dose to the target. Delivering the dose in concave shape and organ sparing are shown in Figure 2.4. This technology also provides dose homogeneity in target and helical Tomo Therapy accomplishes sharp dose gradient. It is possible to treat multiple targets at the same time.<sup>70-71</sup>

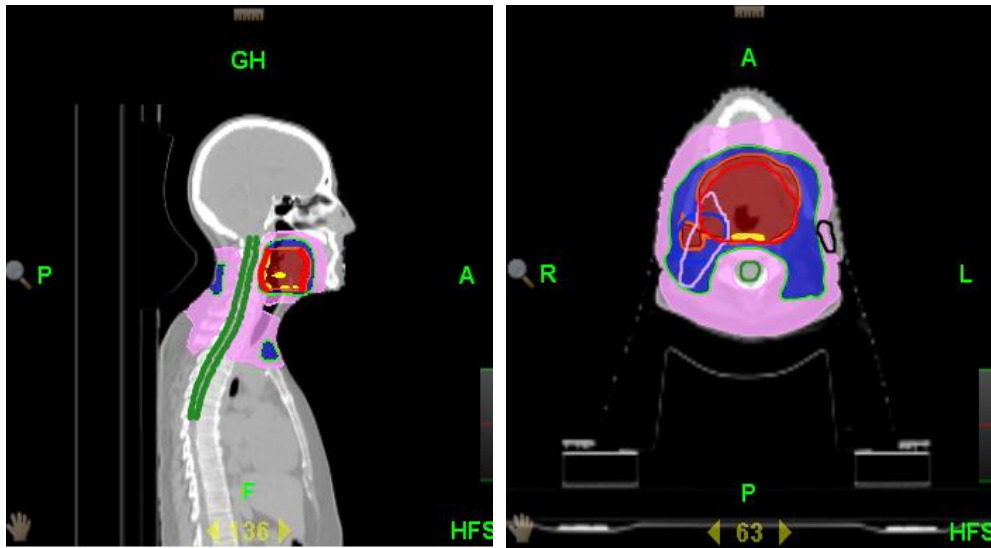


Figure 2.4 Delivering dose in concave shape and organ sparing. PTV1, parotid glands and the cord are shown

The first step of Tomo Therapy planning is target delineation. Before the image guidance technology, all targets had the expansion around the CTV to prevent irradiation for normal tissues due to organ motion. After image guidance radiation therapy began to use to determine deformation and organ motion, reducing the margin became possible.

Therefore, using helical Tomo Therapy while delivering the treatment can provide target volume contraction accuracy.<sup>72</sup>

For this study, all PTV, CTV and critical structures were contoured as usual. PTV1 was determined as a target. It includes gross tumor volume and CTV1. To prevent setup errors, PTV1 has maximum 5mm margin around CTV surface. Usually all planning target volumes have expansions. Since daily kVCT images were obtained during the treatment course, clinical target volume was used as a main target. The targets and the critical structures were contoured slice by slice on kVCT images. The purpose of using CTV as a target reduces toxicity for critical structures especially for parotid glands. Irradiation of parotid glands causes xerostomia for head and neck cancer patients.<sup>73</sup> Therefore, this research aims to protect OARs by planning the treatment by using CTV instead of PTV. While doing the target delineation, radiation oncologists have to be careful to prevent overlaps. However, it is usually impossible depending on tumor location. If tumor abuts the

critical structures, especially parotid glands, these organs can overlap on to clinical target volume. At that time, parotid glands receive a higher dose than the actual planned one. Even though this overlapping occurs, one of the parotid glands can be spared. It is sufficient to produce saliva to increase quality of life for patients.<sup>74</sup>

Helical Tomo Therapy planning is similar to IMRT treatment planning. Inverse planning is also used for helical Tomo Therapy but a rotational gantry system and binary multi-leaf collimator are promoted instead of a fixed number of beam angles. Therefore the planned dose is delivered to the target in helical mode while the couch moves longitudinally. The irradiation of normal tissues is prevented with this way.<sup>70</sup> Since Tomo Therapy uses multi-leaf collimator, complete blocking is possible with Tomo Therapy software system. It is important to protect critical structures because other fan beams cannot send the radiation to the blocked area. It provides a better organ sparing while delivering the radiation in concave shape to the target. On the other hand, blocking provides in-homogenous dose coverage for target. In addition, it causes to deliver a higher dose to the unblocked region.<sup>75</sup> Two steps- pre-calculation and the optimization stages are separated in helical Tomo Therapy planning. A convolution - superposition algorithm provides dose calculation to plan treatment for Tomo Therapy. Some parameters such as field width, pitch and modulation factor are important for Tomo Therapy planning. The field width can be 1cm, 2.5 cm, 5 cm and it is the thickness of the fan beam. To accomplish a high dose fraction, field width has to be bigger than 1 cm. The pitch is the ratio between couch and field width.<sup>32</sup>

There are three options for pitch;

- ✓ Pitch 1: Fine
- ✓ Pitch 2: Normal
- ✓ Pitch 3: Course

These pitch values play a role to change couch velocity. The modulation factor determines the speed of gantry rotation. Plan parameters for the selective cases are shown in Table 2.1. For this research, 2.5 cm was chosen as a field width to provide a high dose fraction. Decreasing the field width and pitch and increasing the modulation factor provide larger

irradiation periods. It means dose distribution can be achieved for tumor, which has a complex shape, with steep dose gradient.<sup>76</sup>

Table 2.1 Plan parameters for the selected case (Patient-4).

## 2.Gy Fraction

| Number of Fractions | Duration (sec) | Gantry Rotations | Gantry Period | Expected MU | Couch Travel (cm) | Couch Speed (cm/sec) | Planned Field Widths |
|---------------------|----------------|------------------|---------------|-------------|-------------------|----------------------|----------------------|
| 35                  | 373.4          | 28.7             | 13.0          | 5.267       | 20.7              | 0.05541              | 9.2                  |

### 2.4.3.1 Optimization

Optimization process begins with positioning the beam angles and beam lets. The beam lets determine the success of the optimization process. To have higher dose conformity, the number of beam lets that can be appropriate for treatment should be excessive.<sup>17</sup> After changing the field width, pitch and modulation factor, optimization is taken into consideration to have better organ sparing. Optimization process is beneficial to attenuate the delivered dose to the critical structures. Also, delivering the actual dose to the target is the most important part of optimization process. Optimization process is executed based on the number of iteration. The process can be controlled by stopping and restarting it. Dose volume histograms can be evaluated with optimization process. While running the process, importance, maximum and minimum dose penalties can have different values. The importance reveals comparative quantity of planning target volume and critical structures. Maximum and minimum penalties show the restriction for critical structures. In this research, it is aimed to increase the homogeneity of delivered dose in target. Therefore, PTV coverage is the most crucial part of optimization process.<sup>8</sup> In addition, the planner considers to constraint organs at risk such as spinal cord, brainstem, and parotid glands. The pulse of radiation coming from the beam is changed by inverse planning system. Also, dose volume histogram is updated throughout optimization process. Dose volume histogram provides useful information about how much dose the relative volume receives. Figure 2.5 shows dose volume histogram received after optimization process.

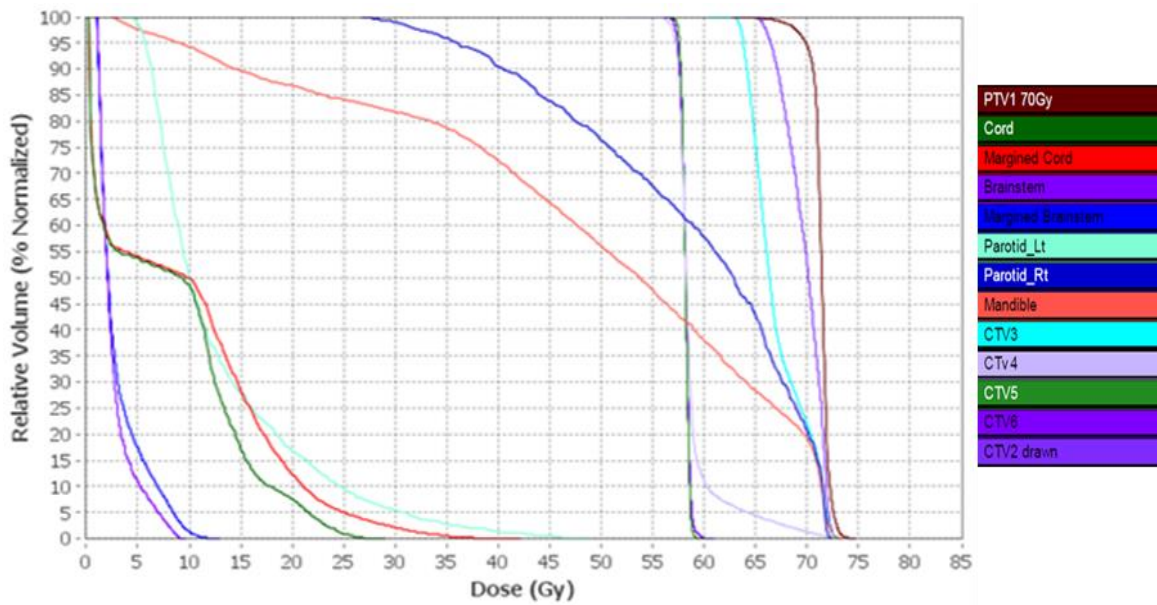


Figure 2. 5 Dose Volume Histogram- Standard Cumulative Mode Relative. 95% of the PTV1 (70 Gy) volume receives at least 70 Gy for the current plan.

If organ sparing and dose homogeneity are satisfying, the planner can stop the optimization process. Before giving the final dose, the system generates a dose calculation. After finishing it, final dose is calculated by the system. As a result Tomo Therapy plan is ready to deliver treatment. <sup>18</sup>



## CHAPTER 3

---

### MATERIALS AND METHODS

#### 3.1 Patient Population and Treatment Planning

Ten H&N cases treated with simultaneous integrated boost on a TomoTherapy unit were retrospectively analyzed (Accuracy Inc., CA). 70% of the patients were diagnosed with malignant neoplasm of tonsil, 10% had nasopharynx cancer and 20% of the patients were diagnosed based of tongue. Patients` characteristics are shown in Table 3.1. The patients` weight was recorded during six to eight weeks. These patients treated with intensity modulated radiation therapy on helical Tomo Therapy unit. During the treatment, a thermal plastic mask was used to provide immobilization. Each patient had one planning CT and daily kVCT images during the 6 to 8 weeks radiation treatment course. Treatment plan was done based on planning CT. Standard protocols were followed for target delineation and contouring the OARs. All targets including PTV1 (gross disease volume), PTV2 (next echelon nodal regions), PTV3 (areas harboring subclinical disease) were delineated on the planning CT regarding other anatomical boundaries of structures. The standard margin plan was generated by giving 3- mm margin to CTV1, CTV2 and CTV3. It was the reference plan. Patients were treated based on this plan. These patients' treatment was re-planned by using 0-mm margin for CTV2 and CTV3. However, standard margin was protected for PTV1. At the same time, daily kVCT images were obtained to correct set-up errors. For helical Tomo Therapy planning system, the field width was determined as 2,5 cm and the pitch value as 0,277. Lastly, the planning modulation factor was chosen as 2,200. The prescription dose was 70 Gy. The treatment was delivered in 35 fractions. Moreover, 62.7 and 56.1 Gy were prescribed for PTV2 and PTV3 respectively.

Table 3.1 The characteristics of patients

| Patient | Diagnosis   | Prescription<br>Dose<br>(Gy) | Tx<br>Duration<br>(Days) | Initial<br>Weight<br>(kg) | Final<br>Weight<br>(kg) | Weight<br>Change<br>(kg) |
|---------|-------------|------------------------------|--------------------------|---------------------------|-------------------------|--------------------------|
| 2       | Tonsil      | 70                           | 53                       | 72.1                      | 63.3                    | -8.8                     |
| 4       | BOT         | 70                           | 51                       | 63.5                      | 62.6                    | -0.9                     |
| 14      | Nasopharynx | 69.96                        | 47                       | 81.6                      | 76.2                    | -5.4                     |
| 21      | Tonsil      | 70                           | 56                       | 95.7                      | 84.8                    | -10.9                    |
| 23      | Tonsil      | 70                           | 39                       | 83.9                      | 76.9                    | -7                       |
| 25      | Tonsil      | 70                           | 50                       | 88                        | 85.9                    | -2.1                     |
| 28      | Tonsil      | 70                           | 43                       | 93.4                      | 83.8                    | -9.6                     |
| 29      | Tonsil      | 70                           | 45                       | 107.5                     | 96                      | -11.5                    |
| 33      | Tonsil      | 66                           | 43                       | 86.4                      | 82                      | -4.4                     |
| 3       | BOT         | 70.2                         | 50                       | 99.8                      | 89.1                    | -10.7                    |

### 3.2 Optimization Process Based on Zero-Margin

These patients were treated on the basis of the first plan (standard margin plan). Since image guidance allows reducing the margin for the optimization process, the treatment was re-planned with CTV as a target instead of PTV. However, 3 mm margin of PTV1 was saved to provide tumor coverage. As a result, the new plan was generated based on 0-mm margin to give the same dose as the original plan to the target while minimizing the delivered dose for critical structures.

In the second step, the pitch value and the field width were chosen as the same value with the actual plan. It was assured that the red lasers were located correctly based on BBs. After making sure of these steps, the optimization process was started. For each structure, approximately 100- 120 iterations were accepted. And then, maximum dose, minimum dose and mean dose were compared with the actual planned dose for target and critical structures. If the value of composite dose of this structure was smaller than the actual delivered dose, calculating the final dose ended the optimization process. On the other hand, if the values of maximum dose, minimum dose and average dose were higher than the actual planned dose, the optimization was repeated by changing some parameters such

as importance, maximum dose penalties and minimum dose penalties. For some important structures, higher importance was given to obtain a good optimization. After changing the parameters, the process was run again and then the planned dose was compared with the standard margin plan. The final dose calculation was acquired to complete the optimization based on the clinical target volume (CTV). Eventually, the new dose- volume histogram was obtained. The planned dose regarding standard margin plan and 0-mm margin plan are shown in Table 3.2 and Table 3.3. PTV1, CTV2-3, cord and parotid glands were taken into consideration for data analysis.

Table 3.2 Plan parameters based on standard margin plan

| <b>Standard Margin Plan</b> |                 |                  |                  |                  |                  |                  |                  |                     |                      |
|-----------------------------|-----------------|------------------|------------------|------------------|------------------|------------------|------------------|---------------------|----------------------|
| <b>Patient</b>              | <b>PTV1</b>     |                  | <b>CTV2</b>      |                  | <b>CTV3</b>      |                  | <b>Cord</b>      | <b>Left Parotid</b> | <b>Right Parotid</b> |
|                             | <b>Max (Gy)</b> | <b>Ave. (Gy)</b> | <b>Max. (Gy)</b> | <b>Ave. (Gy)</b> | <b>Max. (Gy)</b> | <b>Ave. (Gy)</b> | <b>Max. (Gy)</b> | <b>Ave. (Gy)</b>    | <b>Ave. (Gy)</b>     |
| <b>2</b>                    | 76.69           | 71.83            | 74.43            | 72.25            | 74.0             | 72.29            | 41.51            | 22.4                | 38.88                |
| <b>4</b>                    | 74.39           | 71.01            | 73.36            | 71.82            | 72.4             | 67.67            | 41.83            | 24.02               | 61.41                |
| <b>14</b>                   | 74.45           | 71.37            | 73.55            | 66.05            | 72.9             | 66.99            | 33.22            | 56.42               | 49.19                |
| <b>21</b>                   | 74.22           | 72.07            | 73.7             | 70.39            | 62.36            | 57.71            | 44.91            | 62.98               | 23.37                |
| <b>23</b>                   | 74.11           | 70.99            | 72.92            | 71.07            | 72.68            | 69.22            | 39.65            | 60.93               | 24.55                |
| <b>25</b>                   | 77.93           | 71.13            | 75.03            | 68.02            | 70.90            | 64.23            | 39.63            | 24.85               | 24.56                |
| <b>28</b>                   | 73.99           | 71.43            | 73.99            | 71.7             | 73.48            | 67.7             | 43.39            | 40.98               | 14.02                |
| <b>29</b>                   | 76.47           | 71.56            | 76.47            | 69.05            | 73.3             | 59.13            | 44.32            | 27.48               | 22.92                |
| <b>33</b>                   | 69.33           | 67.31            | 68.93            | 66.61            | 68.93            | 58.91            | 42.71            | 7.56                | 38.83                |
| <b>34</b>                   | 74.16           | 71.14            | 73.01            | 67.02            | 72.12            | 61.99            | 40.18            | 22.76               | 20.81                |
| <b>Mean</b>                 | 74.43           | 70.98            | 73.54            | 69.39            | 71.28            | 64.58            | 35.03            | 41.13               | 31.85                |

Table 3.3 Plan parameters based on 0-mm margin plan.

| <b>0-mm Margin Plan</b> |                 |                  |                  |                  |                  |                  |                  |                     |                      |
|-------------------------|-----------------|------------------|------------------|------------------|------------------|------------------|------------------|---------------------|----------------------|
| <b>Patient</b>          | <b>PTV1</b>     |                  | <b>CTV2</b>      |                  | <b>CTV3</b>      |                  | <b>Cord</b>      | <b>Left Parotid</b> | <b>Right Parotid</b> |
|                         | <b>Max (Gy)</b> | <b>Ave. (Gy)</b> | <b>Max. (Gy)</b> | <b>Ave. (Gy)</b> | <b>Max. (Gy)</b> | <b>Ave. (Gy)</b> | <b>Max. (Gy)</b> | <b>Ave. (Gy)</b>    | <b>Ave. (Gy)</b>     |
| <b>2</b>                | 74.65           | 71.68            | 72.46            | 70.11            | 71.78            | 68.75            | 38.11            | 19.55               | 29.35                |
| <b>4</b>                | 74.61           | 71.35            | 72.8             | 69.79            | 73.06            | 67.15            | 29.06            | 13.09               | 59.03                |
| <b>14</b>               | 73.57           | 69.85            | 72.81            | 67.06            | 71.27            | 65.16            | 27.77            | 51.34               | 48.92                |
| <b>21</b>               | 75.45           | 72.48            | 75.06            | 70.38            | 61.59            | 57.81            | 34.7             | 58.71               | 19.37                |
| <b>23</b>               | 78.26           | 71.27            | 72.03            | 68.98            | 73.25            | 69.2             | 29.35            | 57.01               | 14.14                |
| <b>25</b>               | 76.38           | 70.9             | 77.55            | 67.79            | 69.83            | 63.91            | 36.73            | 21.03               | 19.90                |
| <b>28</b>               | 76.21           | 71.35            | 73.96            | 71.24            | 72.35            | 66.81            | 38.68            | 40.83               | 12.72                |
| <b>29</b>               | 77.0            | 71.86            | 76.76            | 69.11            | 73.96            | 59.1             | 41.24            | 26.52               | 21.16                |
| <b>33</b>               | 71.6            | 67.84            | 70.31            | 66.77            | 69.95            | 59.15            | 43.89            | 6.87                | 37.68                |
| <b>34</b>               | 73.87           | 71.43            | 73.48            | 66.93            | 72.56            | 62.04            | 39.53            | 21.24               | 12.85                |
| <b>Mean</b>             | 75.3            | 70.95            | 73.81            | 69.01            | 70.78            | 64.09            | 35.5             | 31.61               | 27.52                |

### 3.3 Deformable Image Registration

Pretreatment kilo voltage CT for target delineation and daily kilo voltage CT to correct set-up error were obtained before the treatment. Resizing and resampling of CT images were done for the registration process. In order to obtain kV-to-kV registration, alignment was done manually. The main concern of the registration process was to provide a close overlaid for two scans as much as possible. As a result, daily kVCT was resampled. GPU algorithm helped to contribute a suitable match to the planning CT resolution. Among the advantages of GPU algorithm are the use of texture memory and the combination of the three dimensional linear interpolation. Anatomical changes were tracked by using deformable image registration. Deformable image registration algorithm was developed by

Anand Santhanam and Yugang Min<sup>78</sup>. An optical flow was employed for this algorithm. Deformation vectors were obtained based on each Cartesian direction. The smoothing factor, the number of levels, the number of warps and the maximum number of iterations are known as registration parameters. 5 levels, 2 warps, and 150 iterations were applied for this study. Jacobian analysis was performed for deformed anatomy. In order to determine non rigid- change in the patient- setup, deformation based on each contoured structure was evaluated. U, V and W matrices were used for Jacobian determinant for each voxel. The determinant is defined by

$$J_i = \begin{vmatrix} \left(\frac{dU}{dx}\right)_i & \left(\frac{dU}{dy}\right)_i & \left(\frac{dU}{dz}\right)_i \\ \left(\frac{dV}{dx}\right)_i & \left(\frac{dV}{dy}\right)_i & \left(\frac{dV}{dz}\right)_i \\ \left(\frac{dW}{dx}\right)_i & \left(\frac{dW}{dy}\right)_i & \left(\frac{dW}{dz}\right)_i \end{vmatrix} \quad (3.1)$$

For this study, 6 to 8 kVCTs were selected for each patient. These kVCTs were superimposed on to the planning CT images. Targets and OARs volume were re-outlined on each kVCT images automatically. The doses were then recalculated from each kVCT to determine actual delivered dose to the targets and the critical structures. The cumulative dose was calculated by summing, week by week, to give total calculated dose. To make a comparison between the accumulated dose and the planned dose, Gamma analysis was performed. Based on our model, all patients were treated identically and the change in the anatomy was not considered for dose distribution. For Gamma analysis, 1% and 1 mm was chosen as the default criteria. The equation for gamma calculation is defined by

$$\Gamma(\vec{r}_e, \vec{r}_r) = \sqrt{\frac{r^2(\vec{r}_e, \vec{r}_r)}{\Delta d^2} + \frac{\delta^2(\vec{r}_e, \vec{r}_r)}{\Delta D^2}} \quad (3.2)$$

### 3.4 Data Analysis

In order to determine whether or not there is a difference between the standard margin plan

and the 0- mm margin plan, effective size test was done for the first data analysis. Effective size test is defined by the difference in two mean doses and dividing this by average standard deviation.

$$\text{Effective Size} = \frac{\text{Average of the post mean dose} - \text{Average of the pre mean dose}}{\text{Average Standard deviation}} \quad (3.3)$$

All targets, parotid glands, and cord were regarded to analyze whether there is a correlation or not for planned dose between both plans. There are three different levels based on this test result; significant difference, middle difference, and low difference. And then basic comparison was made based on the graphics to observe how much difference have been obtained between maximum dose, minimum dose and average dose regarding the standard margin plan and the 0- mm margin plan. Instead of all structures, some critical structures such as parotid glands and cord have been taken into consideration for this step.

The delivered dose was evaluated regarding center of mass (COM) displacement by using the GPU based 3D image framework, which allows the real time dose accumulation and evaluation. The correlation between COM and the delivered dose was evaluated based on the results. In order to determine whether the delivered dose is affected by COM displacement or not, a basic comparison was made between the ratio of the composite dose and the planned dose, and the change in COM displacement based on initial location and final location. In addition, the volume contraction for targets and parotid glands were studied for each patient to determine the change over time. This change was compared with the original volume at the time of planning. A basic comparison was done for the dose changes over time.

## CHAPTER 4

---

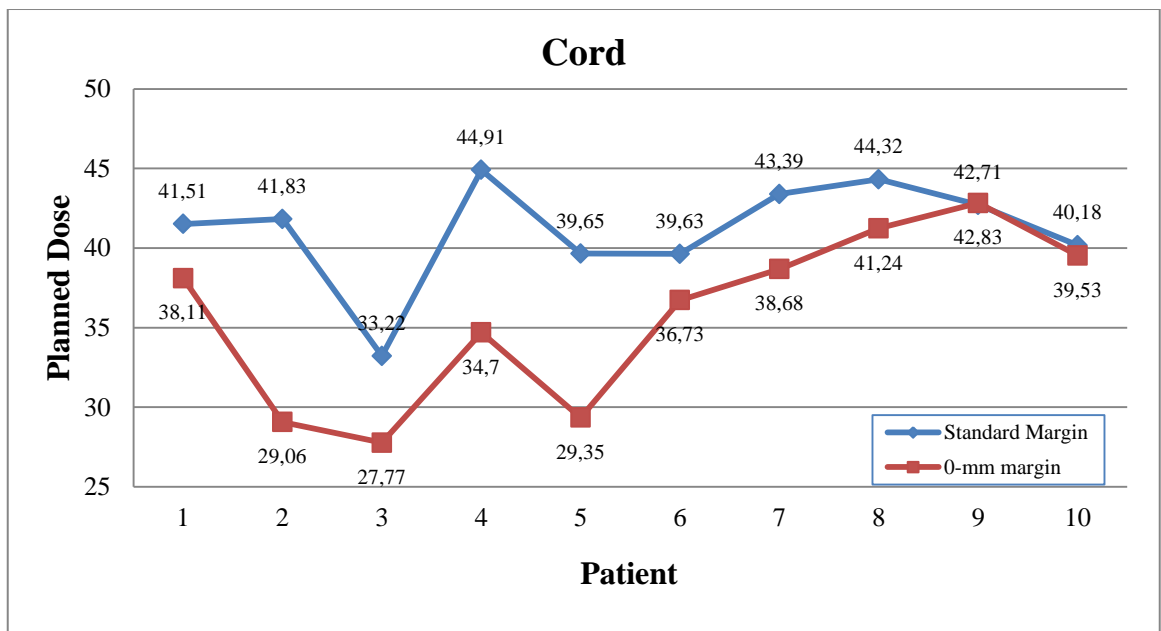
### RESULTS

#### 4.1.1 Effective size test results

The planned dose and weekly delivered dose were studied based on two different plans (standard plan and 0-mm margin plan) by using GPU- based image framework. This technique allows us to evaluate real time dose accumulation. Spinal cord, parotid glands, PTV1, CTV2 and CTV3 were considered. According to the literature, a threshold for parotid glands determines that the xerostomia will become permanent. If the delivered dose to parotid glands is approximately 25- 30 Gy for the mean dose or 30 Gy for the dose received by  $\geq 50$  % of the parotid volume, xerostomia will become permanent. Summary of dosimetric parameters of the standard margin plan and the 0-mm margin plan is shown in Table 3.2 and Table 3.3. The average planned dose from ten patients based on the standard margin plan is 35.03 and 31.85 for left and right parotid glands respectively. However, the average planned dose from ten patients based on the 0-mm margin plan is 31.61 and 27.52 for left and right parotid glands. In order to detect whether there is statistical difference between the standard margin plan and the 0-mm margin plan or not, effective size test was employed for this research. If the test results are higher than 0.6, the difference between two plans is significant. If the range is between 0.6 and 0.27, medium difference is obtained. If the range is smaller than 0.27, the difference between two plans is not significant. Based on the effective size test result, 1.04 for maximum dose of spinal cord was obtained. The difference between the standard margin plan and the 0-mm margin plan was crucial for the cord. Reducing margins will improve the sparing of the cord by  $\approx 23\%$ . Maximum difference was taken into consideration.

The average dose was considered for parotid glands. The test result was 0.32 and 0.11 for right parotid gland and left parotid gland respectively. As a result, medium difference was obtained for the right parotid gland.

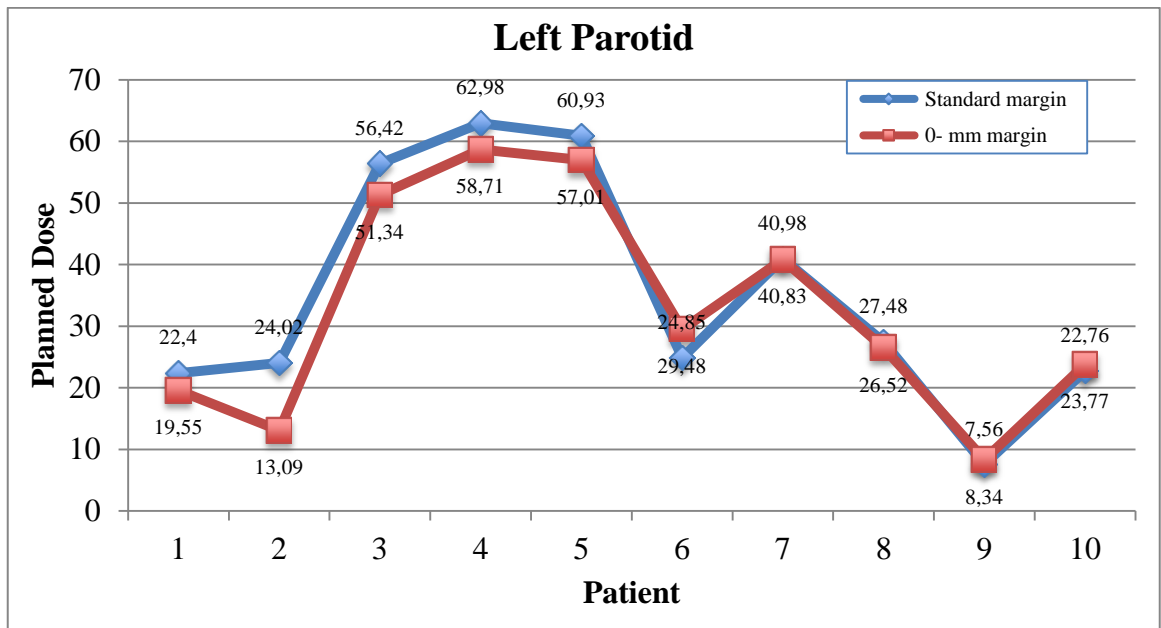
On the other hand, there was no crucial difference in the planned dose of left parotid gland. Reducing margin will improve sparing by  $\approx 16.5\%$  and  $9\%$  for right parotid gland and left parotid gland respectively. As a result, the difference in the planned dose regarding the standard margin plan and 0-mm margin plan was  $15.5\%$  for the cord,  $14.7\%$  for right parotid gland,  $2.76\%$  for left parotid gland. Since the location and the size of tumor affect the planned dose and the delivered dose, fewer doses were tried to be planned to protect the critical structures. The planned dose for critical structures regarding standard margin plan versus 0-mm margin plan is shown in Figure 4.1.



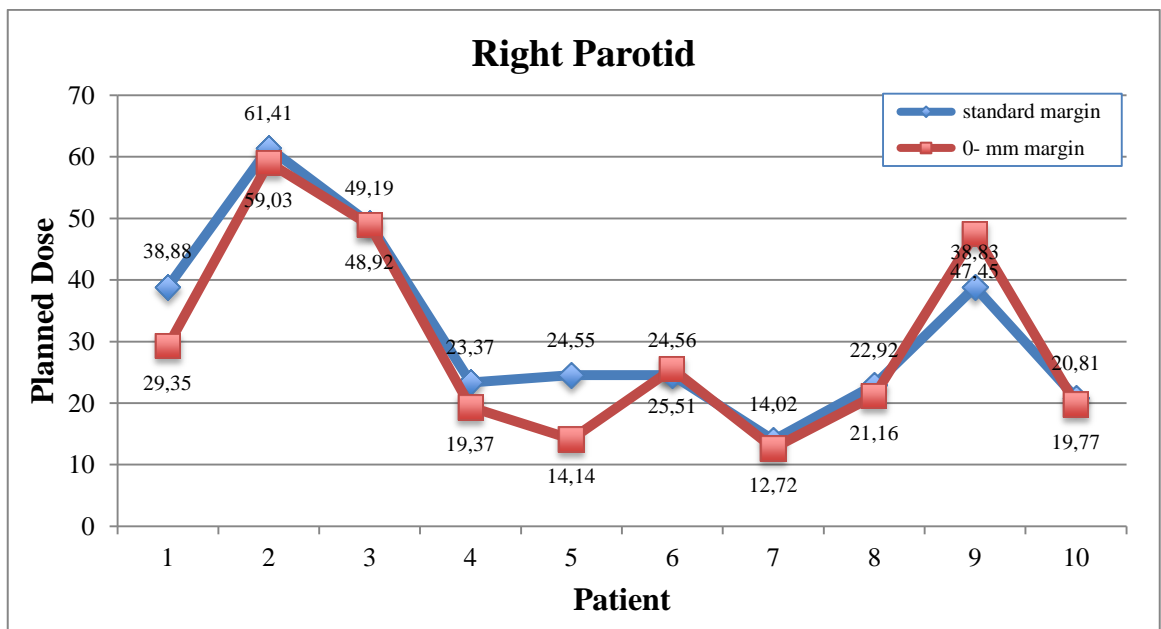
(a)

Figure 4.1 The planned dose for critical structures regarding standard margin plan versus 0-mm margin plan (a) Cord planned dose (b) Left parotid planned dose (c) Right parotid planned dose





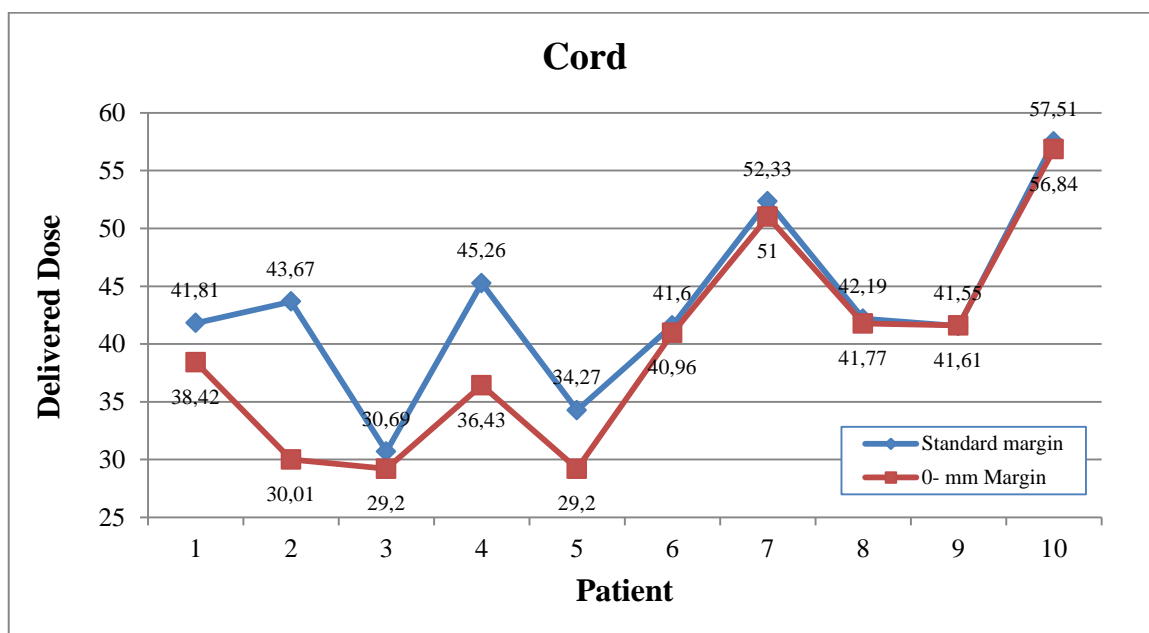
(b)



(c)

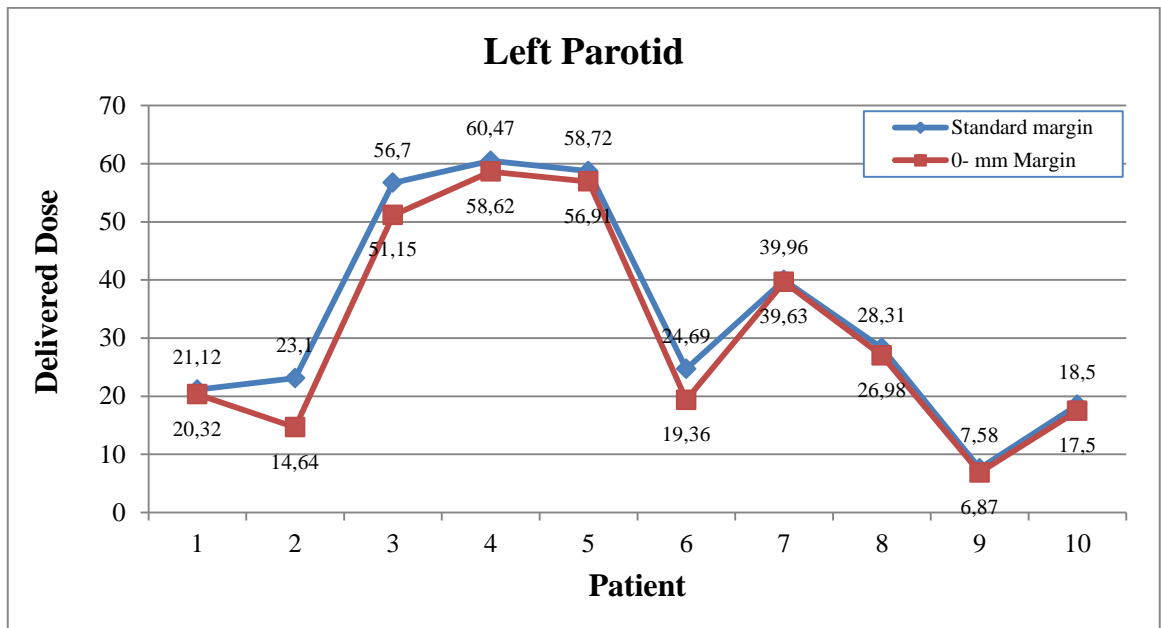
Figure 4.1 (continue) The planned dose for critical structures regarding standard margin plan versus 0- mm margin plan (a) Cord planned dose (b) Left parotid planned dose (c) Right parotid planned dose

After delivering the treatment, the delivered dose was compared based on the standard margin plan and the 0-mm margin plan. The difference in the delivered dose regarding standard margin plan and 0- mm margin plan was  $\approx 10\%$  for the cord,  $\approx 8\%$  for the left parotid gland,  $\approx 19\%$  for the right parotid gland. The cord received a higher dose than the planned dose with a range of 1 Gy- 15 Gy in 5 patients, when standard margin was employed. However, the cord of 2 patients received a higher dose than the planned dose with an average of 10.5 Gy by the usage of 0-mm margin plan. The delivered dose for critical structures regarding standard margin plan versus 0- mm margin plan is shown in Figure 4.2. Last patient's cord received higher dose than the actual planned dose. This patient lost approximately 10 kilos during the treatment. Because of the anatomical change, this patient's treatment was re-planned after 3<sup>rd</sup> week. But statistical analysis was done based on first plan. The second plan was not considered.

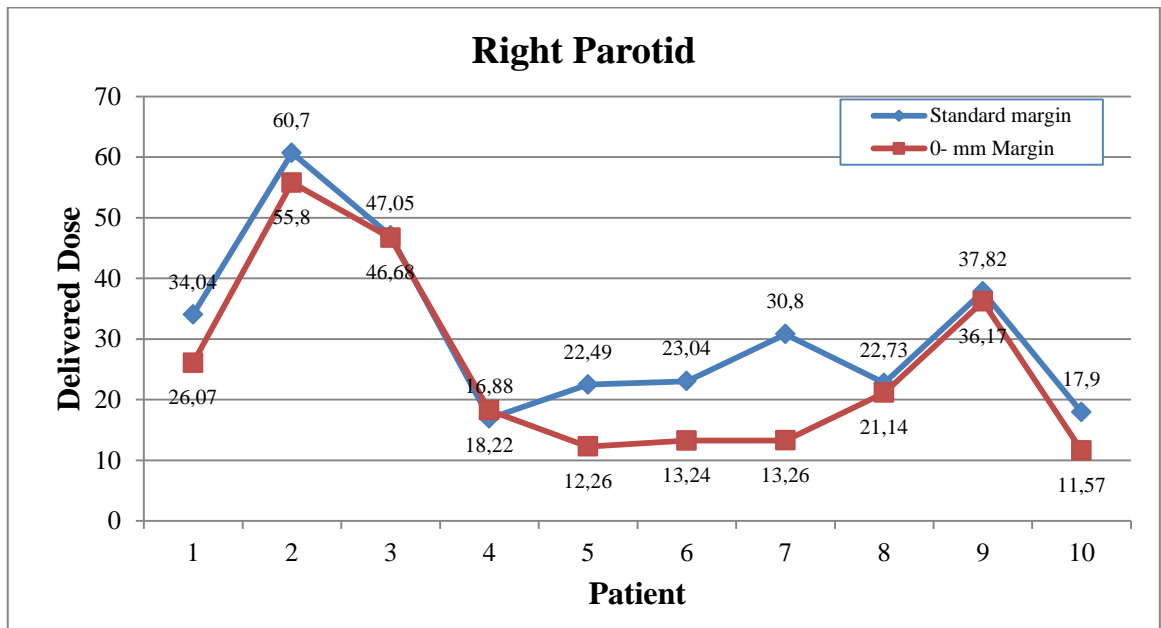


(a)

Figure 4.2 The delivered dose for critical structures regarding standard margin plan versus 0- mm margin plan (a) Cord delivered dose (b) Left parotid delivered dose (c) Right parotid delivered dose



(b)



(c)

Figure 4.2 (continue) The delivered dose for critical structures regarding standard margin plan versus 0- mm margin plan (a) Cord delivered dose (b) Left parotid delivered dose (c) Right parotid delivered dose

One of the purposes of this research is to deliver the same dose to the targets as the planned dose. Although safety margin was reduced to make the high dose region smaller while sparing OARs, it did not affect the delivered dose to the PTV1 and CTVs. The difference in the delivered dose for ROI from 10 patients is shown in Figure 4.3. All results are doses from standard margin plan and 0- mm margin plan, normalized to planned dose of standard margin plan in order to determine whether there is a difference regarding standard margin plan and 0- mm margin plan or not.

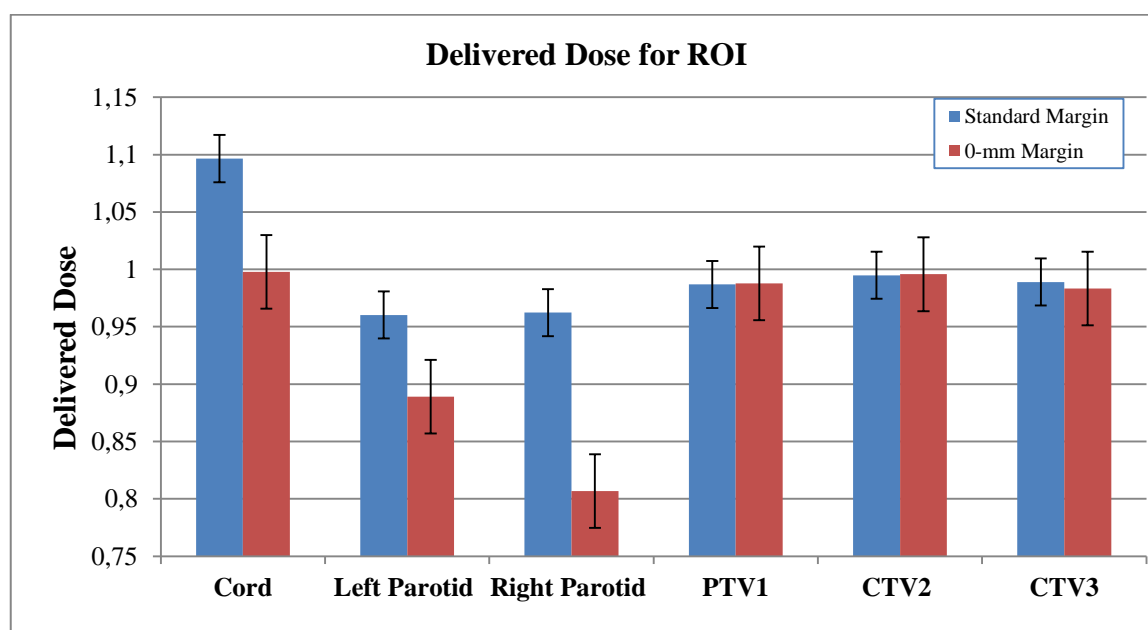


Figure 4.3 The difference in delivered dose for ROI from 10 patients. All results are doses from standard margin plan and 0- mm margin plan, normalized to planned dose of standard margin

#### 4.1.2 The Change in weight, volume and COM displacement

During the treatment course, all patients' weight was recorded every week. Every patient lost weight. Maximum loss in weight was 11 kilos; minimum loss in weight was 2 kilos. It causes the contraction of tumor volume for all cases. That means the initial treated volume was higher than the final treated volume for all patients. In addition, weight loss did not affect volume shrinkage of targets by itself. Since head and neck cancer has a complex

shape and many factors can affect tumor location and size, it is unknown why tumor volume change is not crucial in 2 cases even though these patients lost weight. However, the volume of tumor of patient- 10 decreased significantly during the treatment course because this patient lost 10 kilos during the treatment. The mean volume reduction in PTV1 was 3.3 % with the range of 6.3- 1%. Even though weight loss caused volume shrinkage for some patients, it is a general situation for all cases.

Weight loss affected the volume of parotid glands as well. The volume of right parotid gland was decreased significantly for patients who lost more weight during the treatment course. The mean volume reduction in right parotid gland was 11.7 % with the range of 29.3- 1.3 %. For three patients, weight lost affected the right parotid gland volume. On the other hand, patient-10 lost approximately 11 kilos; the decrease of the volume of right parotid gland was not significant.

The treated volume of left parotid gland fluctuated every week as well. Rises and falls were observed. As a result, volume change was not symmetric for each week. The same result was acquired for the volume of left parotid gland that decreased compared to the initial treated volume and the final treated volume. The mean volume reduction in left parotid gland was 13.5 % with the range of 25.9- 5.7 %. There was not a correlation between weight loss and the decline of parotid gland volume for patient-2. Even though this patient lost approximately 1 kilo during the treatment course, the change in volume was significant. The changes in the volume of CTV2 and CTV3 were evaluated. The mean volume reduction in CTV2 was  $\approx 7$  % with the range of 18 – 0.8 %. The mean reduction in CTV3 volume was 8.6 % with the range of 18 – 5.2 %. The volume change of ROI during the treatment course is shown in Figure 4.4. Average volume change from 10 patients was considered.

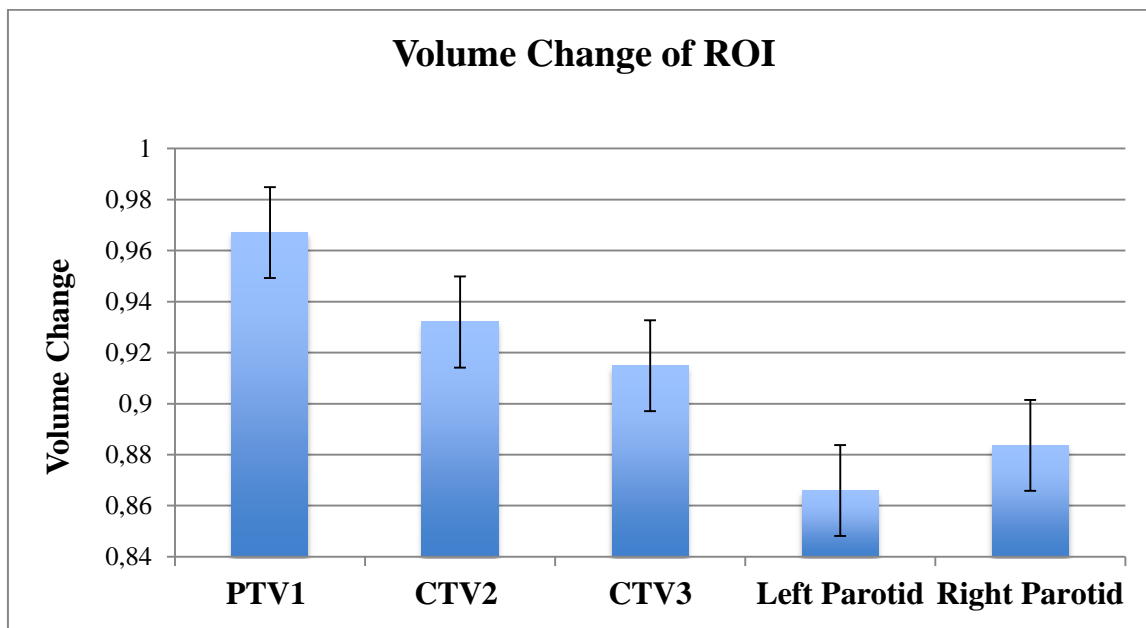


Figure 4.4 Volumetric Changes of ROI from 10 patients during the treatment course. The volumes were normalized to the planning volume. Average volume change was considered. Error bars are standard error.

It was proved that the distance between the right parotid and the left parotid glands was decreased due to anatomical changes. In addition, the decrease in the volume of parotid glands affected the distance between right and left parotid glands. As a result, the location of parotid glands changed. The decline of the distance between parotid glands is shown in Figure 4.5. The distance was calculated according to 3 dimensional Cartesian coordinate system. The mean reduction in the distance between parotid glands was 2.2 % while the range of maximum decrease in the distance between parotid glands was 3- 0.5 %. Moreover, the decrease of the distance between the cord and PTV as well as parotid glands and PTV was calculated according to 3- dimensional and 2 - dimensional Coordinate system. The shift of COM displacement was asymmetric. The maximum shift was 8% and the minimum shift was 3%. Even though the decrease of the distance was milimetric, it caused a change in the delivered dose to the parotid glands because parotid glands entered the high dose region.

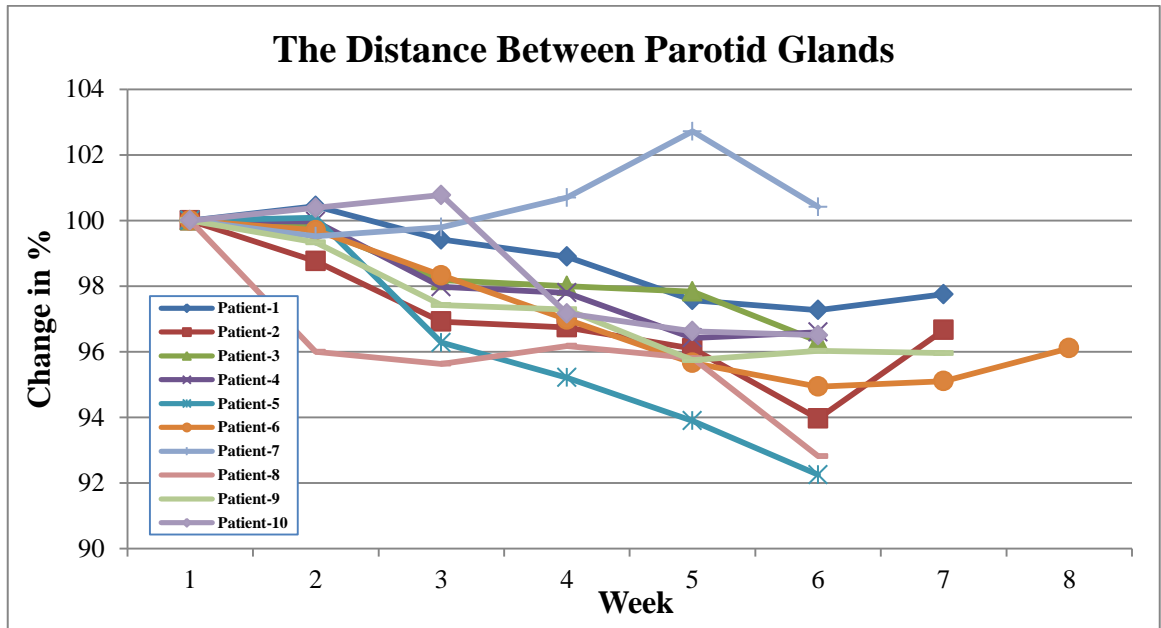


Figure 4. 5 The change in the distance between parotid glands from all patients. The distance was calculated by using 3 dimensional Cartesian coordinate system

#### 4.1.3 Dose comparison between standard margin plan and 0-mm margin plan

Based on Jacobian and Gamma analysis, COM displacement versus delivered dose, accumulated dose versus planned dose and volume change versus delivered dose were evaluated for ROI including targets, cord and parotid glands.

First of all, the accumulated dose was compared with the planned dose for all structures in order to quantify how closely the plan was followed. Weekly kVCT images were used for dose calculation. The delivered dose was corrected depending on the number of fractions for each week. One of the purposes of this research is to deliver the same dose as the actual planned dose to the target. Since  $V_{95}$ , that is the volume (%) of receiving the 95% of the prescription dose, is clinically acceptable for tumor coverage, 95% of the treated volume was considered for this research. The difference in delivered dose between standard and 0-mm margin plan for PTV1 is shown in Figure 4.6. The difference between the planned dose and the delivered dose was  $\approx 2\%$ .  $D_{95}$  based on standard margin plan was  $\approx 4.5\%$

higher for three cases; however, the planned dose was delivered to the PTV1 as expected. Dose discrepancies due to geographic miss were not observed.

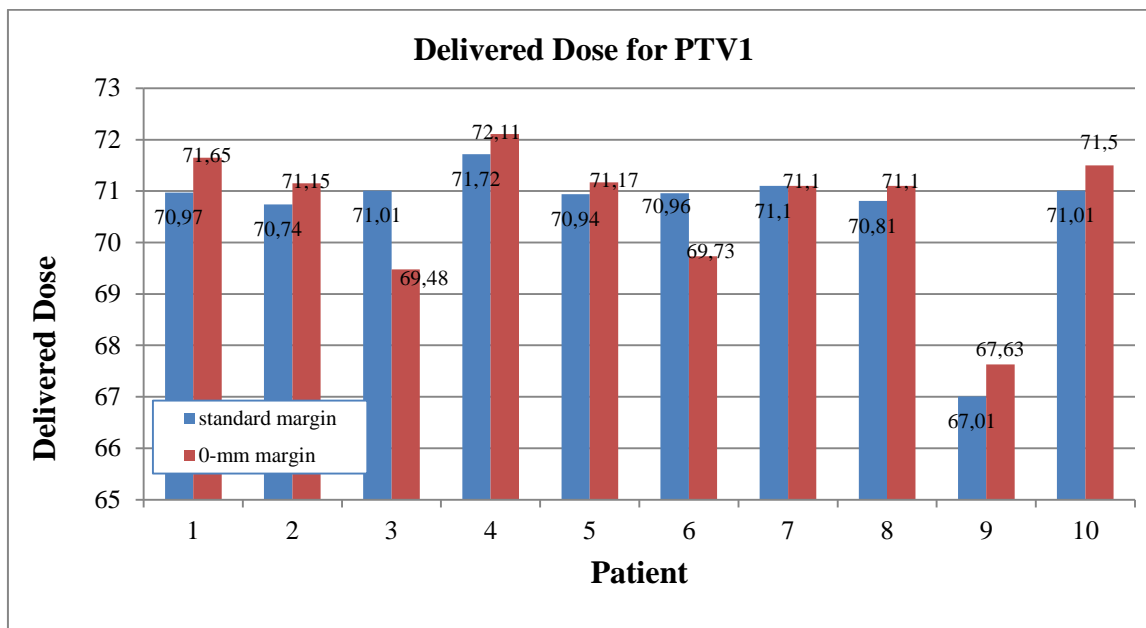


Figure 4.6 The difference in delivered dose between standard and 0-mm margin plan for PTV1

Another purpose of this research is to provide CTV coverage with 0-mm margin plan. PTV1 66.5 Gy was considered for 95% of the treated volume in order to determine the delivered dose based on the standard margin plan and the 0-mm margin plan. The difference in mean dose between standard and 0- mm margin plans for CTV2 is shown in Figure 4.7. D95 was  $\approx 3\%$  higher for 2 cases out of 10 others. This may be caused by the anatomical changes of the CTV. On the other hand, the difference between standard margin and 0- mm margin plans was  $\approx 1\%$ . CTV2 received the same dose as the original plan. A similar result was obtained for CTV3. Dose discrepancies were not observed. The same dose was delivered with 0- mm margin plan. The difference in mean dose between standard margin and 0-mm margin plans for CTV3 is shown in Figure 4.8.



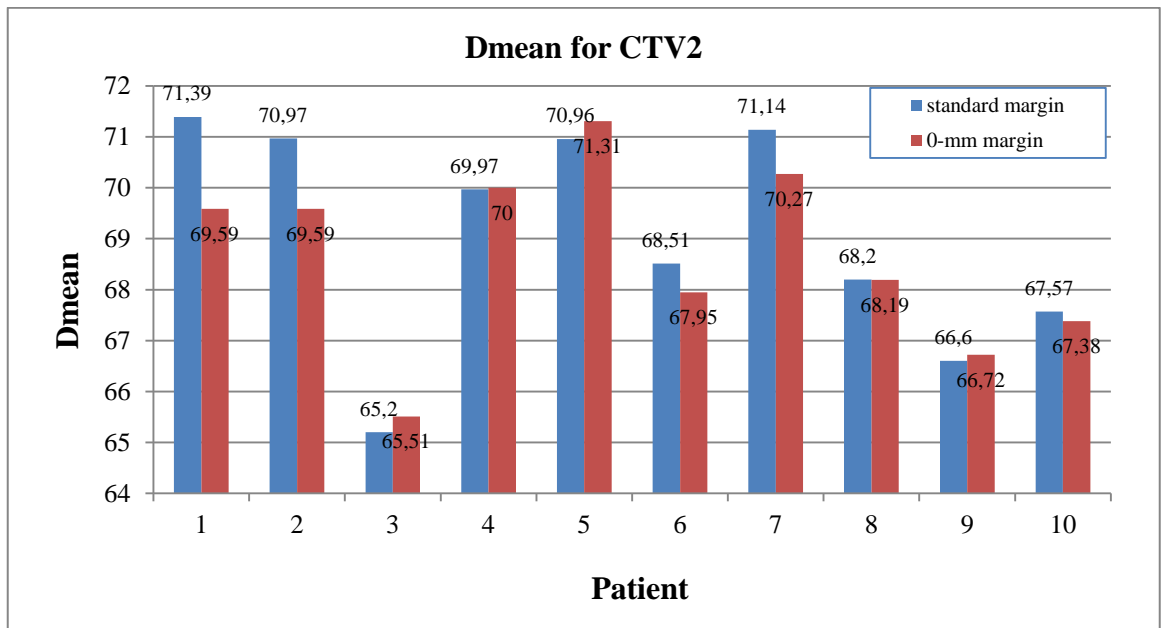


Figure 4.7 The difference in mean dose between standard and 0- mm margin plans for CTV2

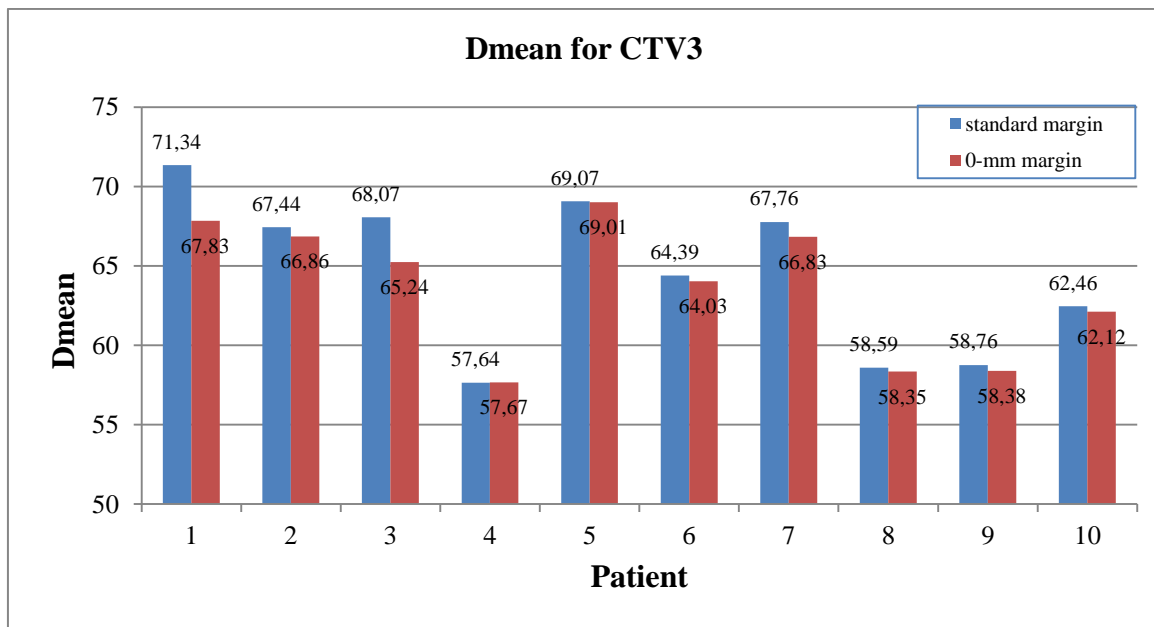


Figure 4.8 The difference in mean dose between standard margin and 0-mm margin plans for CTV3

D95 based on margin plan was  $\approx 5\%$  higher for patient-1 and  $\approx 4.5\%$  higher for patient-3. However, D95 for CTV3 was nearly 100%. In addition, the difference in mean dose between standard margin and 0- mm margin plans was  $\approx 1.5\%$ . Even though safety margin was reduced, 0- mm margin did not affect the delivered dose to the targets. In addition to the delivered dose, 95 % of the treated volume was taken into consideration in order to determine how much tumor coverage was provided. The dosimetric effect of different margins for targets is shown in Figure 4.9. All results are parameters from both plans, normalized to the planned parameters. There was no significant difference between the standard and 0- mm margin plans regarding V95. However, one patient's PTV1 received  $\approx 12\%$  less dose than the planned dose due to anatomical changes. Giving additional margin or re-planning the treatment regarding anatomical changes was necessary for this patient. On the other hand, tumor coverage was provided for 9 cases.

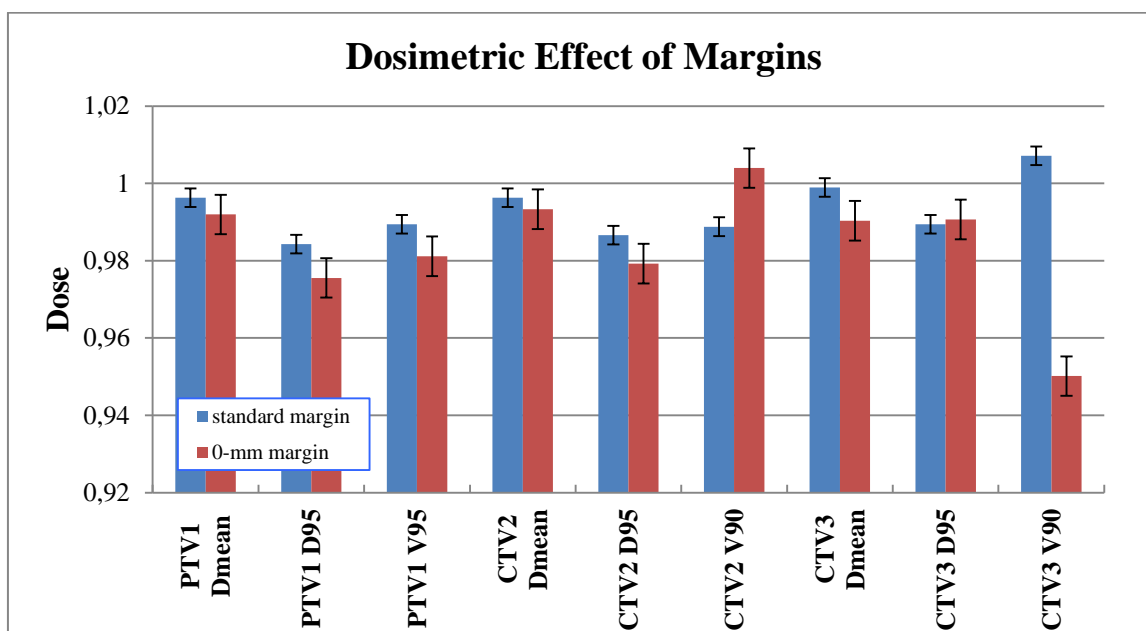


Figure 4.9 The dosimetric effect of different margins for targets

In addition to the delivered dose, 95 % of the treated volume was taken into consideration in order to determine how much tumor coverage was provided. Since tumor coverage was important with the usage of 0- mm margin for level 2 and level-3 planning target volume,

V90 was studied for CTV2 and CTV3 as well. The difference in V90 based on 0-mm margin plan was  $\approx 2\%$  higher than standard margin plan for CTV2 and  $\approx 5\%$  less than standard margin plan for CTV3. V90 received the planned dose as expected. As a result, tumor coverage was provided for targets. Therefore, reducing margin did not affect delivered dose to the targets. Tumor coverage and weekly delivered dose for the selective cases are shown in Figure 4.10.

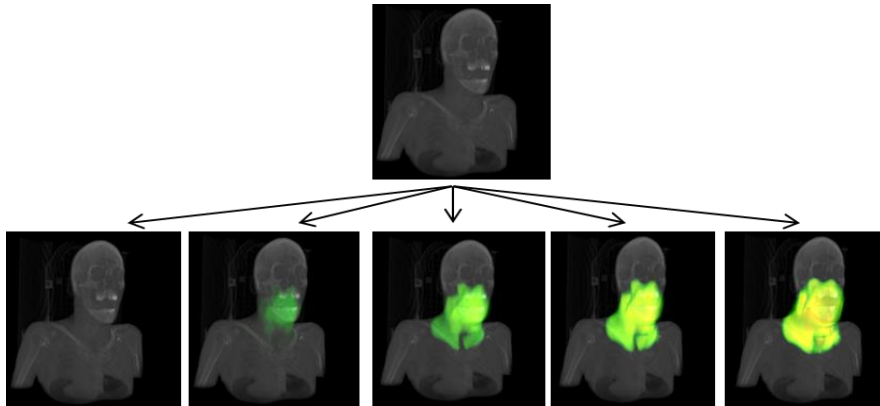
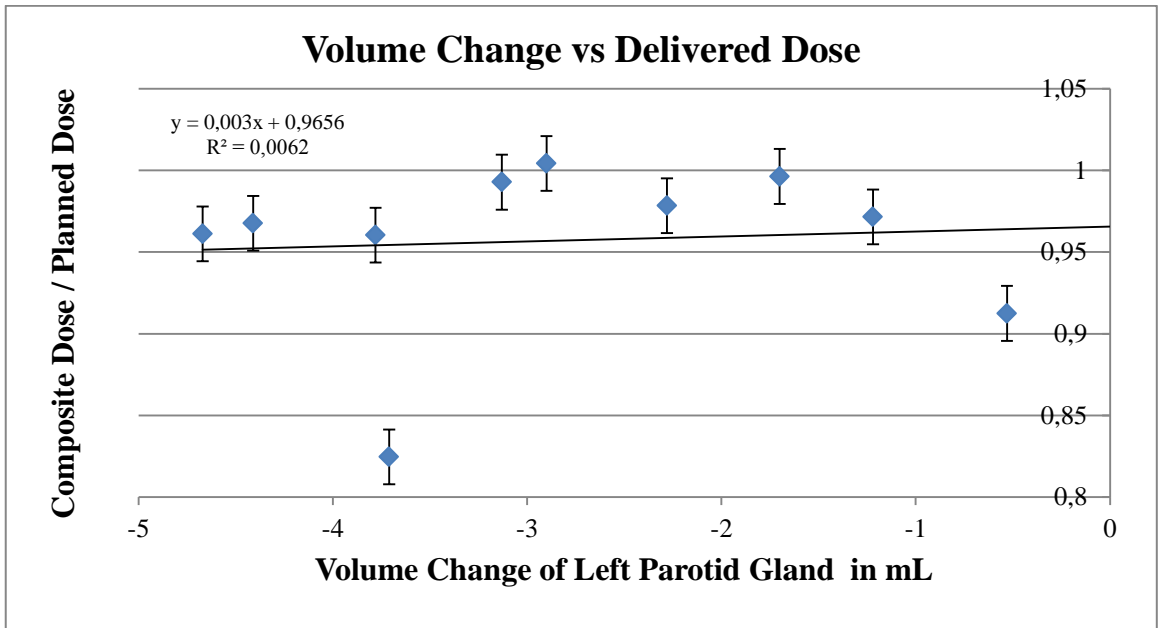
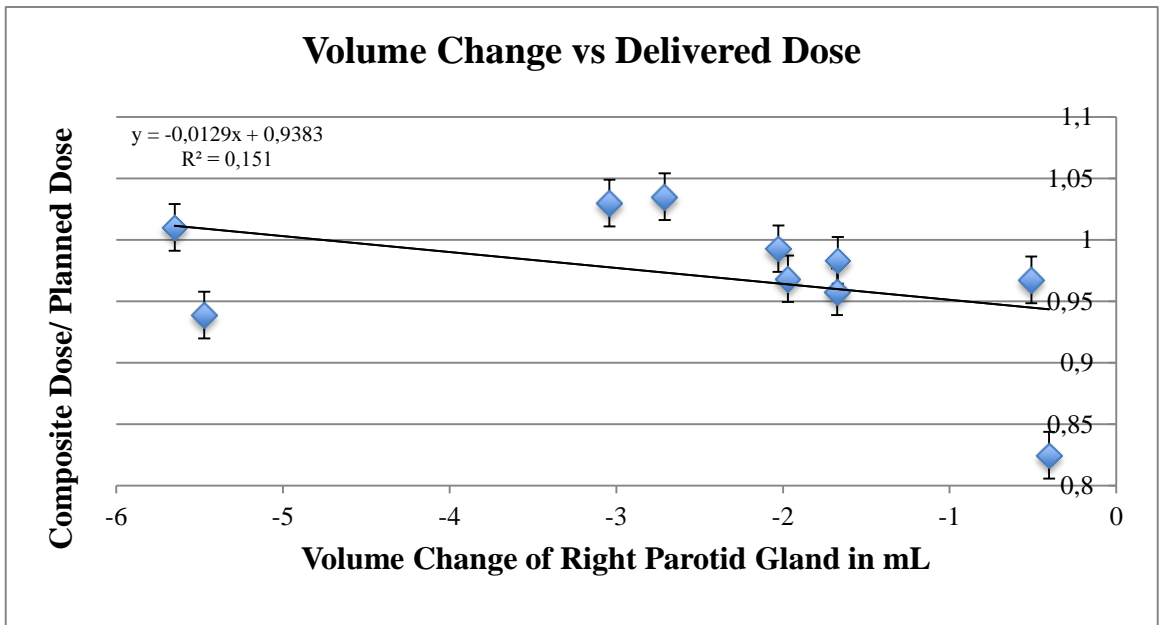


Figure 4.10 Tumor coverage and weekly delivered dose during 6 weeks of the treatment course for selected case. (Patient-3)

One major problem regarding the parotid gland is the volume contraction. Since head and neck cancer patients undergo many anatomical changes during the treatment course, these changes cause the volume contraction of parotid glands as well as targets. In addition, the change in body fluid mass affects the volume of this structure. Even though the volume contraction is small for these structures, it affects their the delivered dose. There is an inverse relationship between the delivered dose and volume contraction. Parotid gland volume decreased during the treatment course, however, the dose that was received by parotid gland increased for some cases. As a result, it can affect patient's quality of life because xerostomia is related to radiation toxicity because radiation toxicity affects the function of parotid glands. The volume change versus delivered dose to right parotid gland and left parotid gland are shown in Figure 4.11.



(a)



(b)

Figure 4.11 (a) The volume change versus delivered dose for left parotid gland  
(b) The volume change versus delivered dose for right parotid gland. Error bars are standard

In our cases, left parotid gland shrank during the treatment course. The delivered dose was not affected by the volume change of left parotid gland. There was not a significant correlation between volume changes versus delivered dose for left parotid ( $R^2= 0.00622$ ,  $R= 0.0788$ ). However, delivered dose was higher in 5 patients. On the other hand, the delivered dose to left parotid gland was less than the planned dose in 2 patients. There was a decrease in the delivered dose to the right parotid gland. The correlation between the changes in the volume of right parotid gland versus delivered dose was not crucial while it was higher than the correlation that was done for left parotid gland ( $R^2= 0.15098$ ,  $R= 0.388$ ). Even though there was decrease in the delivered dose, the right parotid gland received a higher dose in 5 patients. Like the left parotid gland, the delivered dose to right parotid was less than the planned dose in 2 patients. The dose distribution based on standard and 0- mm margin plans is shown in Figure 4.12 for the selected case.

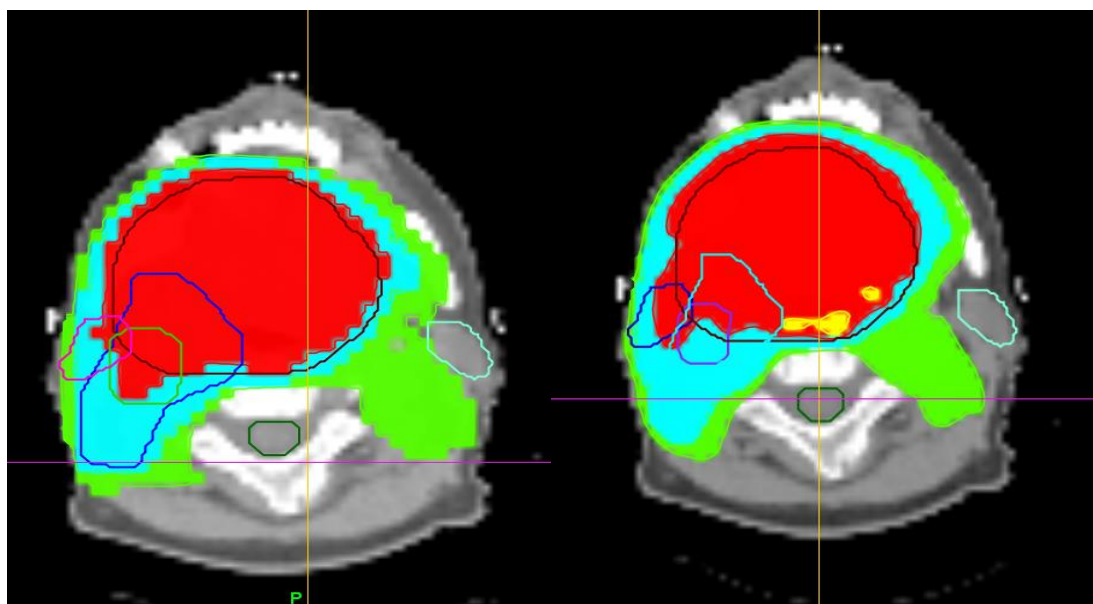


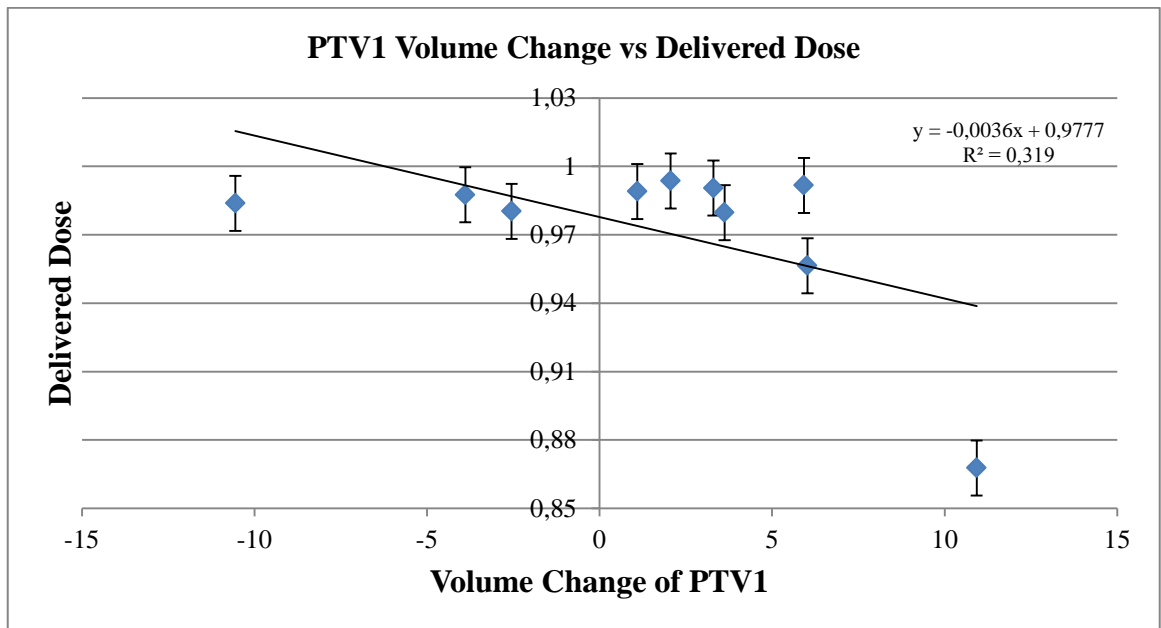
Figure 4.12 The dose distribution based on the standard margin plan and 0-mm margin plans for selected case respectively (Patient-4). (Red= Prescription dose- 70 Gy. Blue= 63 Gy Green= 57 Gy)

Even though 0- mm margin plays a significant role to make high dose region smaller, it is not sufficient to deliver less dose to the OARs. As a matter of fact, the volume of both parotid glands decreased during the treatment course; it is not the only factor that affects the delivered dose to the parotid gland. Tumor location is also essential for the given dose to the critical structure. Another reason why the parotid glands received a higher dose is the change in volume of tumor and the change in the COM of PTV. Since tumor was located so close to the parotid glands in the head and neck region, these changes affected the dose that was received by parotid glands.

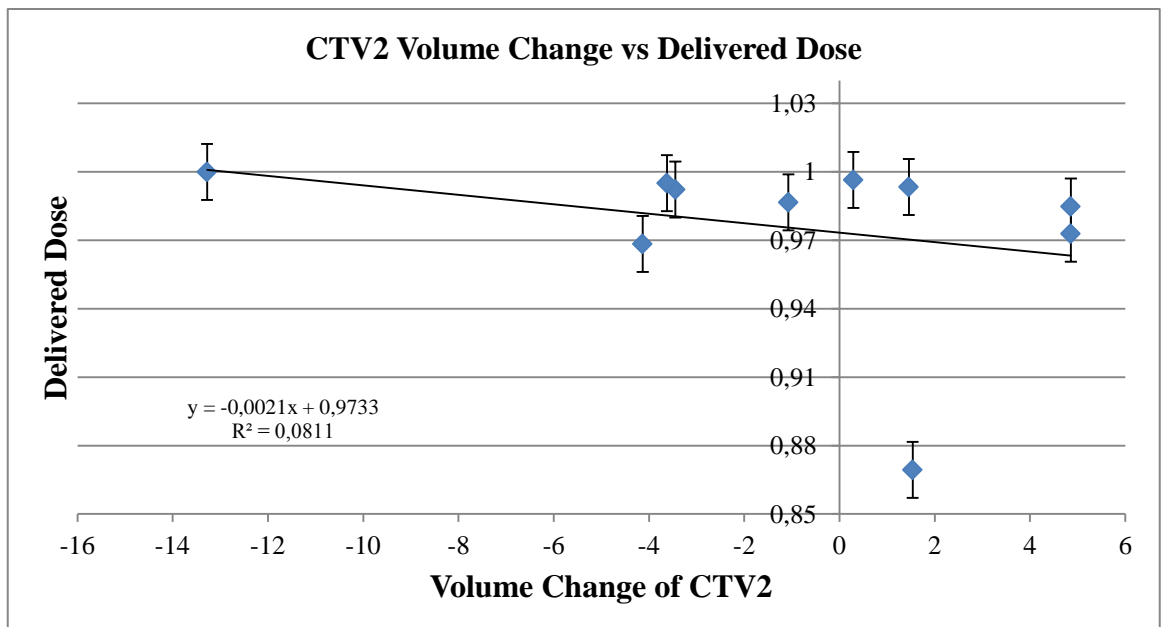
As mentioned above, tumor shrinkage during the treatment course can be observed. In our patients, the volume of PTV1 shrank with the range of 2 mL- 13 mL in all patients. Therefore, there was a decrease regarding delivered dose versus the change in volume of PTV1 ( $R^2= 0.319$ ). The volume change for CTV2 and CTV3 was studied. The volume of CTV2 shrank with the range of 1 mL- 14 mL. Even though CTV2 volume changed during the treatment course, the delivered dose to CTV2 was not affected by the volume change. There was no crucial correlation regarding delivered dose versus volume change ( $R^2= 0.0811$ ). However, the delivered dose to CTV2 was higher than planned dose in 7 patients. In addition, CTV2 received 14 % less dose in one patient.

The similar results were obtained for CTV3. The volume of CTV3 shrank with the range of 3mL- 13mL. Although there was a small increase in delivered dose versus volume change, the correlation was not significant. The delivered dose was higher than the planned dose in 6 patients. On the other hand, CTV3 received 9 % less dose than the planned dose in one patient. The change in volume versus delivered dose for targets is shown in Figure 4.13.

It was proved that the volume of parotid glands shrank during the treatment course. However, center of mass displacement was asymmetric. Based on the initial and final location of parotid glands, the delivered dose increased. There was no correlation between volume change and COM displacement. Since each patient had different anatomical changes, generalization of COM displacement was impossible. It is known that the distance between parotid glands decreased, even though the COM displacement was not symmetric.

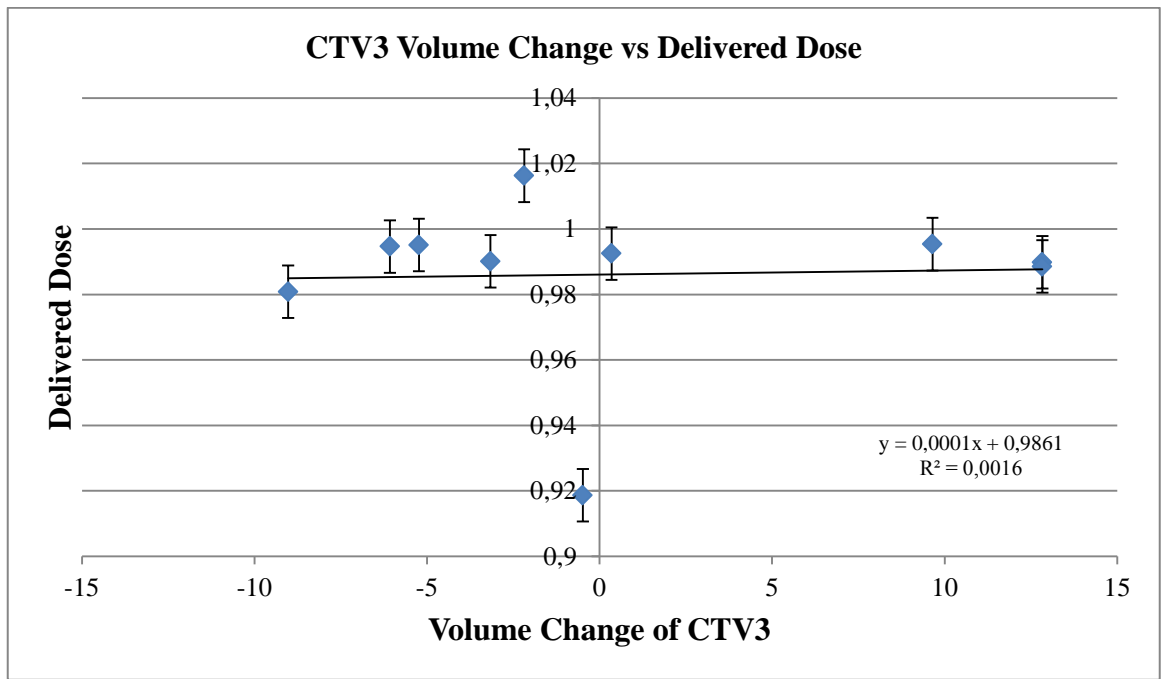


(a)



(b)

Figure 4.13 (a) The change in volume versus delivered dose for PTV1 (b) The change in volume versus delivered dose for CTV2 (c) The change in volume versus delivered dose for CTV3



(c)

Figure 4.13 (continue) (a) The change in volume versus delivered dose for PTV1 (b) The change in volume versus delivered dose for CTV2 (c) The change in volume versus delivered dose for CTV3. All doses are from 0- mm margin plan, normalized to planned dose. Standard error bars were used.

As a result, there was an increase in the delivered dose to the critical structure including the cord ( $R^2 = 0.31651$ ). COM displacement affected the delivered dose to the cord. The cord received an average of 12 % higher dose than the planned dose in 4 patients. The cord of the rest of the patients received the average of 4.5 % less dose than the planned dose. The change in COM displacement versus delivered dose for the cord is shown in Figure 4.14. In addition, the change in distance between parotid glands caused them to enter the high dose region. Thereafter, left parotid gland received a higher dose than the original plan.

The correlation regarding delivered dose versus COM displacement of left parotid gland was less than the correlation made for the cord and. ( $R^2 = 0.2188$ ). Based on the change in COM displacement, the left parotid gland received a higher dose than the planned dose with the range of 5% - 11 % in 5 patients.



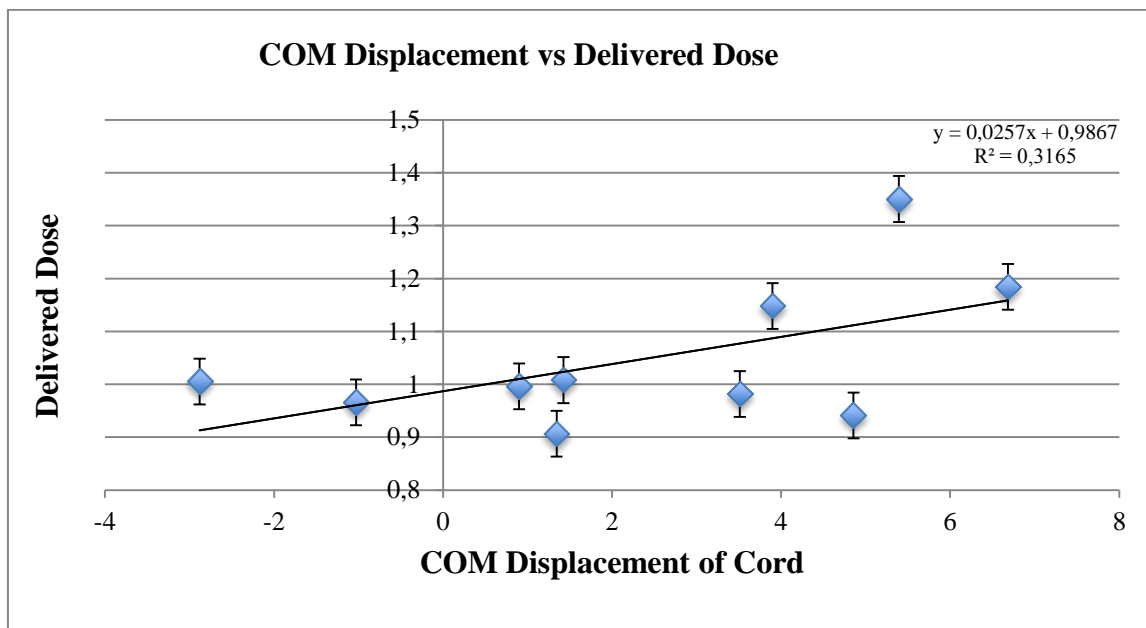
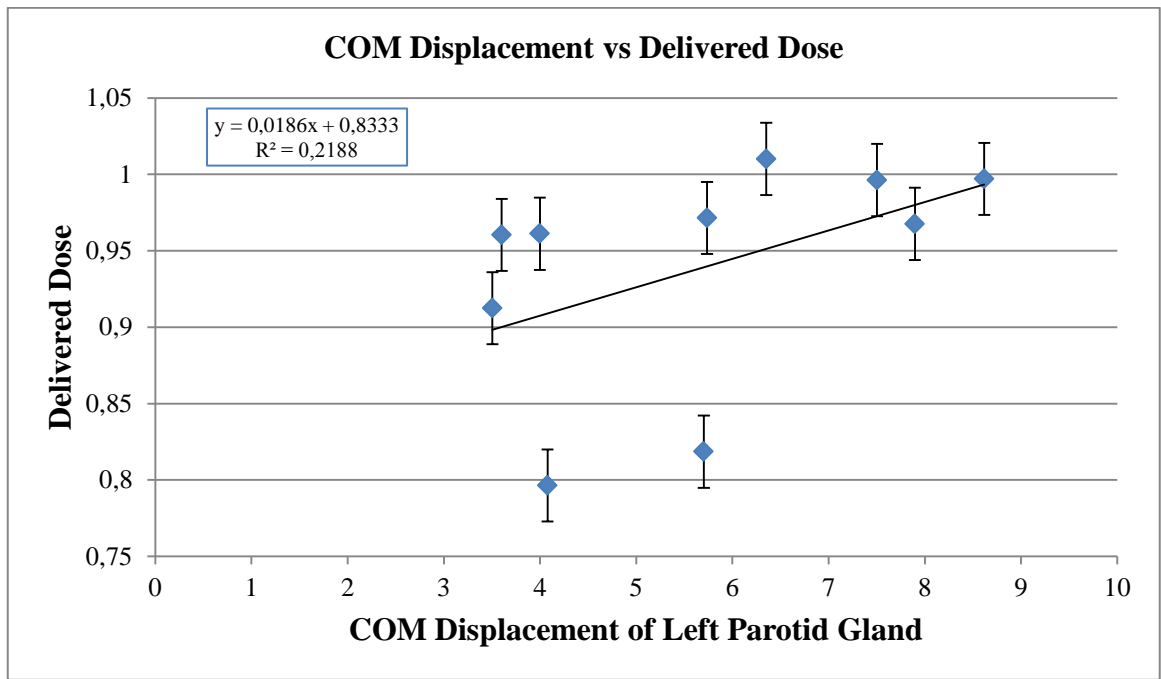


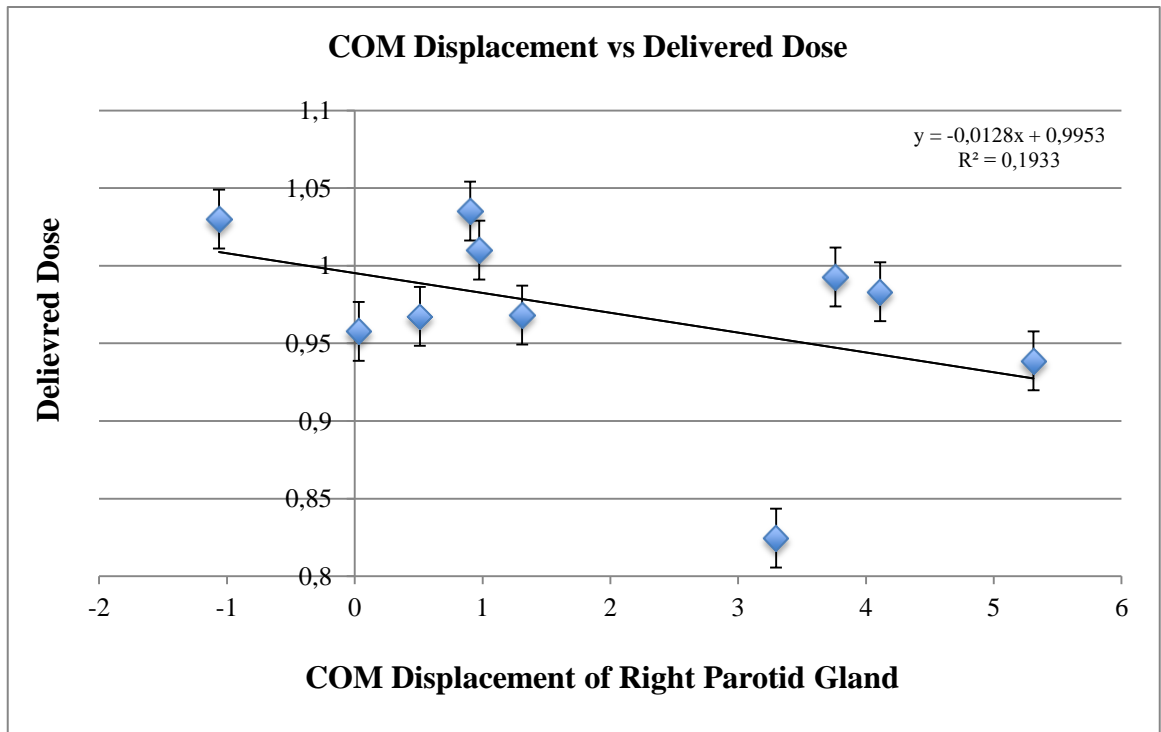
Figure 4.14 The change in COM displacement versus delivered dose for the cord

On the other hand, the delivered dose was  $\approx 10\%$  less than the planned dose in 2 patients. There is a decrease regarding delivered dose versus COM displacement for right parotid gland ( $R^2 = 0.19332$ ). On the other hand, the delivered dose to the right parotid gland was  $\approx 5\%$  higher than the planned dose in 5 patients. The right parotid glands of two patients received an average of 18.5% less dose than the planned dose. The change in COM displacement versus delivered dose for parotid glands is shown in Figure 4.15.

In addition to the change in COM displacement, the distance between parotid glands and PTV1 as well as the distance between the cord and PTV1 were calculated. The distance between the cord and PTV1 decreased in 3 patients. Even though the change in distance was small, it caused the cord to receive a higher dose. Because of this change, there was a small increase in the delivered dose. ( $R^2 = 0.1287$ ). The delivered dose was higher with the average of 16% in 3 patients. On the other hand, the delivered dose to the cord based on the standard margin plan was higher than 0- mm margin plan.



(a)



(b)

Figure 4.15 (a) The change in COM displacement versus delivered dose for left parotid.  
 (b) The change in COM displacement versus delivered dose for right parotid.

Reducing margin was essential to protect critical structures for some cases. As a result, IGRT allows to track anatomical changes. In this study results, volume contraction and COM displacement were evaluated. There were crucial changes in the patient`s anatomy; however, tumor coverage was provided with 0-mm margin. Reducing margin was important for the protection of critical structures, however, they can receive higher dose than actual planned dose under certain circumstances. Giving additional margin to critical structures was not necessary. Tumor coverage was provided for PTV1 and CTV2-3 with the usage of 0- mm margin. Re-planning the treatment due to the change in each patient`s anatomy was necessary for the protection of OARs in some cases. In this study, 3 patients needed adaptive radiation therapy regarding the change in the volume and COM displacement to provide better protection against radiation toxicity.

## **DISCUSSION**

In this study, the standard margin plan was compared to the 0-mm margin plan. It was determined whether IGRT was sufficient or not to protect critical structure by reducing margin. In addition, the change in volume of PTV1 and parotid glands were observed during the treatment course. The accuracy of the volume shrinkage for targets and parotid gland was evaluated. The distance between parotid glands and the distance between the cord and PTV1 were calculated by 3- dimensional Cartesian coordinate system. The distance between parotid glands as well as between the cord and PTV1 decreased during the treatment course. Based on these changes, the planned dose and the delivered dose of the original plan were compared to the 0-mm margin plan. Moreover, the effect of reducing margin was studied by using GPU- based image framework for this thesis. This is capable of calculating real time dose verification and accumulation. One of the goals in this research is to provide tumor coverage to deliver highly conformal radiation dose to the target. Even tough 0-mm margin was employed for this study tumor coverage was provided for PTV1 and CTV2-3. Moreover, it was proved that reducing margin is essential to reduce the delivered dose to the cord. However, it is not enough to protect both parotid glands in all cases. Since head and neck cancer patients undergo many anatomical changes such as weight loss and change in body fluid mass, it affects the treated volume of tumor.

In addition, these anatomical changes caused to the distance to be reduced between parotid glands. As a result, delivered dose to critical structures was higher than the planned dose for some cases. To protect critical structures and to cover 95 % of treated volume of tumor, giving additional safety margin would be necessary. However, the more the treated volume expands the high dose region the more beneficial IGRT is to track tumor and set-up error. Making high dose region smaller became possible by reducing margin with IGRT. In this study, high dose region was made smaller with 0-mm margin plan. This fact is important to deliver fewer doses to the cord and brain stem. In addition, at least one of the parotid glands was protected. One parotid gland received a higher dose than the original plan in three patients. In addition, cord of two patients received higher dose. Not only margin but also tumor location and size are important for the delivered dose. The planned dose of parotid glands was less than the original plan, however, the delivered dose to the left parotid gland is higher, because the tumor mostly was located on the left side of head and neck region in our cases. Besides, the change in volume of parotid glands affected the delivered dose. In these patients, volume of both parotid glands and PTV1 volume decreased during the treatment course. The COM displacement is another crucial factor on delivered dose to the critical structures. Since the distance between left and right parotid glands decreased, it caused the parotid glands enter the high dose region. Therefore, at least one of the parotid glands received a high dose than planned dose based on dose distribution. On the other hand, the insignificant correlation between COM displacement and delivered dose to the critical structures including parotid glands and the cord could be obtained because only 10 cases were analyzed for this research. But, when case-by-case investigation was taken into consideration, a strong correlation was observed between weekly delivered dose and COM displacement.

Many researches have been done before regarding reducing margin. Choonik Lee et. al. analyzed the change in parotid gland dose resulting from anatomical changes.<sup>45</sup> For deformable image registration, the daily MVCT images were used. To evaluate daily and accumulated doses, voxel mapping was employed. As a result, 3 out of the 10 patients were estimated to have received 10 % higher dose than the original plan. There was a strong correlation between the COM change of the parotids and the percentage differences

between the plan and the cumulative mean doses. In 2009, a cumulative dose was reported and then adaptive re-planning was compared based on 0-mm, 3-mm, and 5-mm margin.<sup>77</sup> Firstly, dosimetric effect of tumor and normal tissue shrinkage were evaluated. Similar results were obtained. Volume shrinkage did not affect the target dose. But parotid glands received a higher dose when tighter margin was employed. Secondly, the effect of planning margin based on the planning dose was evaluated [ $D_{\text{mean}}(\text{Parotid}) = 35.7 \text{ Gy}$ ]. However, the delivered dose was not taken into consideration. One major problem regarding this research is that most PTVs overlap on to parotid glands, however; non-overlapping parotid glands was represented to be used in IMRT optimization. The entire parotid gland was used in plan evaluation. Therefore, parotid glands received higher dose. Lastly, tumor shrinkage and contour change during radiotherapy was evaluated in 2010.<sup>67</sup> MVCT images were superimposed to planning kVCT. Target volume and OAR were re-outlined on MVCT. The actual delivered dose was taken into consideration based on MVCT images. According to this research result, there was no significant relationship between the percentage volume reduction and the planned dose. While at first sight, those researches had similar results; they were really different from this study. In this study, four variables were compared to evaluate anatomical changes versus dose. Firstly, the planned dose of the standard margin plan was compared to the planned dose of 0-mm margin plan. And then it was compared to the delivered dose for both plans based on real time imaging modalities. However, re-planning the treatment was not employed for this research. Therefore, treatment plans were generated based on planning CT images. The treatment was performed according to this plan. The accumulated dose and the delivered dose of each week were evaluated depending on GPU based -3D image framework. As a result, the difference between delivered dose and planned dose regarding the plans of each week could not be evaluated. Moreover, there were unknown questions regarding uncertainties caused by anatomical changes. Since there is patient instead of illness, further investigation will be done on adaptive radiation therapy and tumor tracking system.

## **CONCLUSION**

IGRT is one of the most effective tools to correct set-up error. This technique allows the planner to reduce margin. As a result, making high dose region smaller is possible. In

addition, GPU- based 3D image framework was crucial to determine the accuracy of the volume contraction for targets as well as parotid glands and COM. In addition it is used for real dose accumulation and evaluation. Head and neck cancers are located in paranasal sinuses, nasal cavity, oral cavity, pharynx and larynx. Since this type of cancer is mostly seen adjacent to the spinal cord, brain stem, parotid glands and optic pathway, reducing margin is especially important to protect the cord and OARs. However, protecting parotid glands is impossible by reducing margin in all cases due to anatomical changes. At least one of them received a higher dose than planned dose, even though 10-mm margin was employed. Head and neck cancer patients undergo many anatomical changes during the treatment course. These changes affect the COM displacement, the distance between parotid glands, the volume of PTV1 and parotid glands, as well as the distance between PTV1 and the cord. Therefore, reducing margin is not enough to protect parotid glands. Adaptive radiation therapy is crucial in view of the change in every patient's anatomy for each week. A better organ sparing can be provided with re-planning the treatment for some cases. As a result, patient's quality of life would be increased.

## REFERENCES

---

- [1] Ozyigit, G., Yang, T., & Chao, K. C. (2004). Intensity-modulated radiation therapy for head and neck cancer. *Current treatment options in oncology*, 5(1), 3-9.
- [2] Yom, S. S., Raben, D., Siddiqui, F., Lu, J. J., & Yao, M. (2012). Skull Base Head and Neck Cancer. In *Stereotactic Body Radiation Therapy* (pp. 267-284). Springer Berlin Heidelberg.
- [3] McMahon, S., & Chen, A. Y. (2003). Head and neck cancer. *Cancer and Metastasis Reviews*, 22(1), 21-24.
- [4] Hong, T. S., Tomé, W. A., & Harari, P. M. (2005). Intensity-modulated radiation therapy in the management of head and neck cancer. In *Squamous Cell Head and Neck Cancer* (pp. 115-124). Humana Press.
- [5] Lee, N., Xia, P., Fischbein, N. J., Akazawa, P., Akazawa, C., & Quivey, J. M. (2003). Intensity-modulated radiation therapy for head-and-neck cancer: the UCSF experience focusing on target volume delineation. *International Journal of Radiation Oncology\* Biology\* Physics*, 57(1), 49-60.
- [6] van Vulpen, M., Field, C., Raaijmakers, C. P., Parliament, M. B., Terhaard, C. H., MacKenzie, M. A., ... & Fallone, B. G. (2005). Comparing step-and-shoot IMRT with dynamic helical tomotherapy IMRT plans for head-and-neck cancer. *International Journal of Radiation Oncology\* Biology\* Physics*, 62(5), 1535-1539.
- [7] Goitein, M. (2008). IMRT and "Optimization". *Radiation Oncology: A Physicist's-Eye View*, 177-210.
- [8] Webb, S. (2006). IMRT delivery techniques. In *Image-guided imrt* (pp. 73-90). Springer Berlin Heidelberg.
- [9] Sheng, K., Molloy, J. A., & Read, P. W. (2006). Intensity-modulated radiation therapy (IMRT) dosimetry of the head and neck: A comparison of treatment plans using linear accelerator-based IMRT and helical tomotherapy. *International Journal of Radiation Oncology\* Biology\* Physics*, 65(3), 917-923.
- [10] Cedric, X. Y., Amies, C. J., & Svatos, M. (2008). Planning and delivery of intensity-modulated radiation therapy. *Medical physics*, 35(12), 5233-5241.
- [11] Webb, S. (2001). *Intensity-modulated radiation therapy*. CRC Press.

- [12] Xiao, Y. (2013). Image-Guided Radiation Therapy (IGRT): kV Imaging. *Encyclopedia of Radiation Oncology*, 343-351.
- [13] Farzan,S (2012). Non-skull base head and neck cancer. *Stereotactic Body Radiation Therapy* (pp.251-265). Springer Berlin Heidelberg.
- [14] Dawson, L. A., & Jaffray, D. A. (2007). Advances in image-guided radiation therapy. *Journal of clinical oncology*, 25(8), 938-946.
- [15] Schwarz, M., Giske, K., Stoll, A., Nill, S., Huber, P. E., Debus, J., ... & Stoiber, E. M. (2012). IGRT versus non-IGRT for postoperative head-and-neck IMRT patients: dosimetric consequences arising from a PTV margin reduction. *Radiat Oncol*, 7(1), 133.
- [16] Warren, W., Grant III, W. H., & Teh, B. S. (2012). Helical TomoTherapy System. In *Stereotactic Body Radiation Therapy* (pp. 67-77). Springer Berlin Heidelberg.
- [17] Beavis, A. W. (2004). Is tomotherapy the future of IMRT?.
- [18] Peñagaricano, J. A., & Papanikolaou, N. (2003). Intensity-modulated radiotherapy for carcinoma of the head and neck. *Current oncology reports*, 5(2), 131-139.
- [19] Grant III, W. H., Butler, E. B., & Verellen, D. (2012). Tomotherapy image guided radiation therapy. In *Technical Basis of Radiation Therapy* (pp. 313-324). Springer Berlin Heidelberg.
- [20] Toledano, I., Graff, P., Serre, A., Boisselier, P., Bensadoun, R. J., Ortholan, C., ... & Lapeyre, M. (2012). Intensity-modulated radiotherapy in head and neck cancer: results of the prospective study GORTEC 2004–03. *Radiotherapy and Oncology*, 103(1), 57-62.
- [21] McMahon, S., & Chen, A. Y. (2003). Head and neck cancer. *Cancer and Metastasis Reviews*, 22(1), 21-24.
- [22] Yartsev, S., Kron, T., & Van Dyk, J. (2007). Tomotherapy as a tool in image-guided radiation therapy (IGRT): current clinical experience and outcomes. *Biomed Imaging Interv J*, 3(1), e17.
- [23] Argiris, A., Karamouzis, M. V., Raben, D., & Ferris, R. L. (2008). Head and neck cancer. *The Lancet*, 371(9625), 1695-1709.
- [24] Jacques, B. (2011). Head and neck cancer multimodality management. (pp.710)



- [25] Marur, S., & Forastiere, A. A. (2008, April). Head and neck cancer: changing epidemiology, diagnosis, and treatment. In *Mayo Clinic Proceedings* (Vol. 83, No. 4, pp. 489-501). Elsevier.
- [26] Shah, J. P., & Lydiatt, W. (1995). Treatment of cancer of the head and neck. *CA: a cancer journal for clinicians*, 45(6), 352-368.
- [27] Chambers, M. S., Garden, A. S., Kies, M. S., & Martin, J. W. (2004). Radiation-induced Xerostomia in patients with head and neck cancer: Pathogenesis, impact on quality of life, and management. *Head & neck*, 26(9), 796-807.
- [28] Leksell, L. (1983). Stereotactic radiosurgery. *Journal of Neurology, Neurosurgery & Psychiatry*, 46(9), 797-803.
- [29] Eshleman, J. S. (2009). A New Tool to Help Fight Cancer—Tomotherapy. *The Journal*, 4(3), 107.
- [30] Webb, S. (2009). Delivery of Intensity-Modulated Radiation Therapy Including Compensation for Organ Motion. In *Radiotherapy and Brachytherapy* (pp. 141-161). Springer Netherlands.
- [31] Chen, A. M., Jennelle, R. L., Sreeraman, R., Yang, C. C., Liu, T., Vijayakumar, S., & Purdy, J. A. (2009). Initial clinical experience with helical tomotherapy for head and neck cancer. *Head & neck*, 31(12), 1571-1578.
- [32] Ploquin, N. P., Bélec, J. G., & Clark, B. G. (2009, January). Dosimetric Comparison between Helical Tomotherapy and Biologically Based IMRT Treatment Planning System for Selected Cases. In *World Congress on Medical Physics and Biomedical Engineering, September 7-12, 2009, Munich, Germany* (pp. 1012-1015). Springer Berlin Heidelberg.
- [33] Goffman, T. E., & Glatstein, E. (2002). Intensity-modulated radiation therapy. *Radiation research*, 158(1), 115-117.
- [34] Blanco, A. I., Chao, K. S., El Naqa, I., Franklin, G. E., Zakarian, K., Vicic, M., & Deasy, J. O. (2005). Dose-volume modeling of salivary function in patients with head-and-neck cancer receiving radiotherapy. *International Journal of Radiation Oncology\* Biology\* Physics*, 62(4), 1055-1069.
- [35] Hong, T. S., Tomé, W. A., Chappell, R. J., Chinnaiyan, P., Mehta, M. P., & Harari, P. M. (2005). The impact of daily setup variations on head-and-neck intensity-modulated radiation therapy. *International Journal of Radiation Oncology\* Biology\* Physics*, 61(3), 779-788.

- [36] Cedric, X. Y., Amies, C. J., & Svatos, M. (2008). Planning and delivery of intensity-modulated radiation therapy. *Medical physics*, 35(12), 5233-5241.
- [37] Chen, A. M., Farwell, D. G., Luu, Q., Donald, P. J., Perks, J., & Purdy, J. A. (2011). Evaluation of the planning target volume in the treatment of head and neck cancer with intensity-modulated radiotherapy: what is the appropriate expansion margin in the setting of daily image guidance?. *International Journal of Radiation Oncology\* Biology\* Physics*, 81(4), 943-949.
- [38] Yang, J. N., Mackie, T. R., Reckwerdt, P., Deasy, J. O., & Thomadsen, B. R. (1997). An investigation of tomotherapy beam delivery. *Medical Physics*, 24(3), 425-436.
- [39] Ruchala, K. J., Olivera, G. H., Kapatoes, J. M., Schloesser, E. A., Reckwerdt, P. J., & Mackie, T. R. (2000). Megavoltage CT image reconstruction during tomotherapy treatments. *Physics in medicine and biology*, 45(12), 3545.
- [40] Lu, W., Olivera, G. H., Chen, Q., Ruchala, K. J., Haimerl, J., Meeks, S. L., ... & Kupelian, P. A. (2006). Deformable registration of the planning image (kVCT) and the daily images (MVCT) for adaptive radiation therapy. *Physics in medicine and biology*, 51(17), 4357.
- [41] Schmitt, D., Albers, D., & Cremers, F. (2009, January). Suitability of the MVCT of TomoTherapy and Siemens Oncor for Treatment Planning. In *World Congress on Medical Physics and Biomedical Engineering, September 7-12, 2009, Munich, Germany* (pp. 252-255). Springer Berlin Heidelberg.
- [42] Chen, A. M., Jennelle, R. L., Sreeraman, R., Yang, C. C., Liu, T., Vijayakumar, S., & Purdy, J. A. (2009). Initial clinical experience with helical tomotherapy for head and neck cancer. *Head & neck*, 31(12), 1571-1578.
- [43] Schreiner, L. J., Kerr, A., Salomons, G., Dyck, C., & Hajdok, G. (2003). The potential for image guided radiation therapy with cobalt-60 tomotherapy. In *Medical Image Computing and Computer-Assisted Intervention-MICCAI 2003* (pp. 449-456). Springer Berlin Heidelberg.
- [44] Meyer, J.L. (2011). *IMRT, IGRT, SBRT: advances in the treatment planning and delivery of radiotherapy*. Karger Publishers
- [45] Lee, C., Langen, K. M., Lu, W., Haimerl, J., Schnarr, E., Ruchala, K. J., ... & Mañon, R. R. (2008). Assessment of parotid gland dose changes during head and neck cancer radiotherapy using daily megavoltage computed tomography and deformable image registration. *International Journal of Radiation Oncology\* Biology\* Physics*, 71(5), 1563-1571.

- [46] Hong, T. S., Tomé, W. A., Chappell, R. J., Chinnaiyan, P., Mehta, M. P., & Harari, P. M. (2005). The impact of daily setup variations on head-and-neck intensity-modulated radiation therapy. *International Journal of Radiation Oncology\* Biology\* Physics*, 61(3), 779-788.
- [47] Suzuki, M., Nishimura, Y., Nakamatsu, K., Okumura, M., Hashiba, H., Koike, R., ... & Shibata, T. (2006). Analysis of interfractional set-up errors and intrafractional organ motions during IMRT for head and neck tumors to define an appropriate planning target volume (PTV)-and planning organs at risk volume (PRV)-margins. *Radiotherapy and oncology*, 78(3), 283-290.
- [48] Ling, C. C., Yorke, E., & Fuks, Z. (2006). From IMRT to IGRT: frontierland or neverland?. *Radiotherapy and oncology*, 78(2), 119-122.
- [49] Verellen, D., De Ridder, M., Linthout, N., Tournel, K., Soete, G., & Storme, G. (2007). Innovations in image-guided radiotherapy. *Nature Reviews Cancer*, 7(12), 949-960.
- [50] Xing, L., Thorndyke, B., Schreibmann, E., Yang, Y., Li, T. F., Kim, G. Y., ... & Koong, A. (2006). Overview of image-guided radiation therapy. *Medical Dosimetry*, 31(2), 91-112.
- [51] Greco, C., & Clifton Ling, C. (2008). Broadening the scope of image-guided radiotherapy (IGRT). *Acta Oncologica*, 47(7), 1193-1200.
- [52] Warlick, W. B. (2008). Image-guided radiation therapy: techniques and strategies. *Community Oncology*, 5(2), 86-92.
- [53] Sterzing, F., Engenhardt-Cabillic, R., Flentje, M., & Debus, J. (2011). Image-guided radiotherapy: a new dimension in radiation oncology. *Deutsches Ärzteblatt International*, 108(16), 274.
- [54] Jaffray, D. A. (2005, July). Emergent technologies for 3-dimensional image-guided radiation delivery. In *Seminars in radiation oncology* (Vol. 15, No. 3, pp. 208-216). WB Saunders.
- [55] Welsh, J. S. (2009). Helical tomotherapy in the community setting: a personal account. *Community Oncology*, 6(10), 463-467.
- [56] Martin, S., & Yartsev, S. (2010). kVCT, MVCT, and hybrid CT image studies—Treatment planning and dose delivery equivalence on helical tomotherapy. *Medical physics*, 37(6), 2847-2854.

- [57] Murthy, V., Master, Z., Gupta, T., Ghosh-Laskar, S., Budrukkar, A., Phurailatpam, R., & Agarwal, J. (2010). Helical tomotherapy for head and neck squamous cell carcinoma: Dosimetric comparison with linear accelerator-based step-and-shoot IMRT. *Journal of cancer research and therapeutics*, 6(2), 194.
- [58] Chung, Y., Yoon, H. I., Kim, J. H., Nam, K. C., & Koom, W. S. (2013). Is helical tomotherapy accurate and safe enough for spine stereotactic body radiotherapy?. *Journal of cancer research and clinical oncology*, 139(2), 243-248.
- [59] Mackie, T. R., Holmes, T., Swerdloff, S., Reckwerdt, P., Deasy, J. O., Yang, J., ... & Kinsella, T. (1993). Tomotherapy: a new concept for the delivery of dynamic conformal radiotherapy. *Medical physics*, 20(6), 1709-1719.
- [60] Bichay, T. J., Chen, C., Davis, S., Kane, J., Klafeta, S., & Meadows, J. (2007, January). TomoTherapy for cranial radiosurgery/radiotherapy. In *World Congress on Medical Physics and Biomedical Engineering 2006* (pp. 1852-1855). Springer Berlin Heidelberg.
- [61] Xu, S., Deng, X., Dai, X., Wang, L., Wang, Y., Xie, C., ... & Gong, H. (2008, January). Quality assurance of helical tomotherapy intensity modulated radiation therapy. In *7th Asian-Pacific Conference on Medical and Biological Engineering* (pp. 447-450). Springer Berlin Heidelberg.
- [62] Ruchala, K. J., Olivera, G. H., Schloesser, E. A., & Mackie, T. R. (1999). Megavoltage CT on a tomotherapy system. *Physics in Medicine and Biology*, 44(10), 2597.
- [63] Yartsev, S., Kron, T., & Van Dyk, J. (2007). Tomotherapy as a tool in image-guided radiation therapy (IGRT): current clinical experience and outcomes. *Biomed Imaging Interv J*, 3(1), e17.
- [64] Crop. (2012). Tomo therapy MVCT dose calculations. *Journal of Applied Clinical Medical Physics*, 13.6.
- [65] Guckenberger, M. (2011). Image-guided Radiotherapy Based on Kilovoltage Cone-beam Computed Tomography a Review of Technology and Clinical Outcome. *European Oncology and Haematology*; 7(2): 121-4
- [66] Park, S., Cheong, K. H., Hwang, T. J., Kang, S. K., Lee, M., Kim, K. J., ... & Cho, K. H. (2010). When Should an Adaptive Plan be Considered for Head-and-neck Cancer Patients Undergoing Tomotherapy Treatment?. *Journal of the Korean Physical Society*, 56(3), 897-904.
- [67] Loo, H., Fairfoul, J., Chakrabarti, A., Dean, J. C., Benson, R. J., Jefferies, S. J., & Burnet, N. G. (2011). Tumour shrinkage and contour change during radiotherapy increase the dose to organs at risk but not the target volumes for head and neck cancer

- patients treated on the TomoTherapy HiArt™ system. *Clinical Oncology*, 23(1), 40-47.
- [68] Lee, C., Langen, K. M., Lu, W., Haimerl, J., Schnarr, E., Ruchala, K. J., ... & Mañon, R. R. (2008). Evaluation of geometric changes of parotid glands during head and neck cancer radiotherapy using daily MVCT and automatic deformable registration. *Radiotherapy and Oncology*, 89(1), 81-88.
- [69] Fiorino, C., Dell'Oca, I., Pierelli, A., Broggi, S., Martin, E. D., Muzio, N. D., ... & Calandrino, R. (2006). Significant improvement in normal tissue sparing and target coverage for head and neck cancer by means of helical tomotherapy. *Radiotherapy and oncology*, 78(3), 276-282.
- [70] Yang, J. N., Mackie, T. R., Reckwerdt, P., Deasy, J. O., & Thomadsen, B. R. (1997). An investigation of tomotherapy beam delivery. *Medical Physics*, 24(3), 425-436.
- [71] Castadot, P., Lee, J. A., Geets, X., & Grégoire, V. (2010, April). Adaptive radiotherapy of head and neck cancer. In *Seminars in radiation oncology* (Vol. 20, No. 2, pp. 84-93). WB Saunders.
- [72] Baisden, J. M., Benedict, S. H., Sheng, K., Read, P. W., & Larner, J. M. (2007). Helical TomoTherapy in the treatment of central nervous system metastasis. *Neurosurgical focus*, 22(3), 1-6.
- [73] Murthy, V., Master, Z., Gupta, T., Ghosh-Laskar, S., Budrukkar, A., Phurailatpam, R., & Agarwal, J. (2010). Helical tomotherapy for head and neck squamous cell carcinoma: Dosimetric comparison with linear accelerator-based step-and-shoot IMRT. *Journal of cancer research and therapeutics*, 6(2), 194.
- [74] Yartsev, S., Kron, T., Cozzi, L., Fogliata, A., & Bauman, G. (2005). Tomotherapy planning of small brain tumours. *Radiotherapy and oncology*, 74(1), 49-52.
- [75] Gurvich, V., & Feygelman, V. (2009, January). Useful Techniques for Tomotherapy Treatment Planning. In *World Congress on Medical Physics and Biomedical Engineering*, September 7-12, 2009, Munich, Germany (pp. 890-892). Springer Berlin Heidelberg.
- [76] Kaiser, A., Schultheiss, T. E., Wong, J. Y., Smith, D. D., Han, C., Vora, N. L., ... & Radany, E. H. (2006). Pitch, roll, and yaw variations in patient positioning. *International Journal of Radiation Oncology\* Biology\* Physics*, 66(3), 949-955.
- [77] Wu, Q., Chi, Y., Chen, P. Y., Krauss, D. J., Yan, D., & Martinez, A. (2009). Adaptive replanning strategies accounting for shrinkage in head and neck IMRT. *International Journal of Radiation Oncology\* Biology\* Physics*, 75(3), 924-932.

- [78] Min, Y., Santhanam, A., Neelakkantan, H., Ruddy, B. H., Meeks, S. L., & Kupelian, P. A. (2010). A GPU-based framework for modeling real-time 3D lung tumor conformal dosimetry with subject-specific lung tumor motion. *Physics in medicine and biology*, 55(17), 5137.

## CURRICULUM VITAE

---

**Name Surname:** Sümeyra Can

**Place and Date of Birth:** Konya, 01/01/1986

**Address:** Meram Yeni Yol Cad. Kasım Halife Sok. No-6 Meram/Konya

**E-Mail:** sumeyracn@gmail.com

**B.Sc.:** Department of Physics Education, Hacettepe University, Ankara, Turkey

**M.Sc.:** Department of Physics Education, Hacettepe University, Ankara, Turkey

Combined BS/MS program

### **Professional Experience:**

Research Assistant: Radiation Oncology Department, University of California- Los Angeles, USA. (2013-2014)

Internship: Gamma Knife Unit, Göztepe Medical Park Hospital, Istanbul, Turkey (2013)

Science Teacher: Diltaş College, Konya, Turkey (2011-2013)

Physics Teacher: Ankara Açı Training Center, Ankara, Turkey (2008-2009)

### **Rewards:**

Fellowship: Institute of Biomedical Engineering, Fatih University, Istanbul, Turkey (2012-2014)

Prof. Dr. İhsan Dođramacı Merit Award Hacettepe University, Ankara, Turkey (2009)

Top Academic Achievement Award: Department of Physics Education, Hacettepe University, Ankara, Turkey . (2009)

### **List of Publications:**

Margin Reduction of Level II/III Planning Target Volume for Image-Guided Simultaneous Integrated Boost Head-and-Neck Treatment (Authors: Sümeyra Can, X. Sharon Qi, Anand Santhanam, John Neylon, Dan Low)

Feasibility of Margin Reduction for Level II and III Planning Target Volume in Head-and-Neck Image guided Radiotherapy (Authors: X. Sharon Qi, Anand Santhanam, John Neylon,

Sümevra Can, Patric Kupelian